

**Integrating Advanced Sizing and Controllability
Assessment Methods into an MDO Framework for
Optimal Redundancy in UAV Design**

Robin Warren

A Thesis

in

The Department

of

Mechanical, Industrial and Aerospace Engineering

Presented in Partial Fulfillment of the Requirements

for the Degree of

Master of Applied Science (Mechanical Engineering) at

Concordia University

Montréal, Québec, Canada

April 2023

© Robin Warren, 2023

CONCORDIA UNIVERSITY

School of Graduate Studies

This is to certify that the thesis prepared

By: **Robin Warren**

Entitled: **Integrating Advanced Sizing and Controllability Assessment Methods
into an MDO Framework for Optimal Redundancy in UAV Design**

and submitted in partial fulfillment of the requirements for the degree of

Master of Applied Science (Mechanical Engineering)

complies with the regulations of this University and meets the accepted standards with respect to originality and quality.

Signed by the Final Examining Committee:

_____ Chair
Dr.

_____ External Examiner
Dr. Yong Zeng

_____ Examiner
Dr. Youmin Zhang

_____ Supervisor
Dr. Jonathan Liscouët

Approved by

Martin D. Pugh, Chair
Department of Mechanical, Industrial and Aerospace Engineering

_____ 2023

Amir Asif, Dean
Faculty of Engineering and Computer Science

Abstract

Integrating Advanced Sizing and Controllability Assessment Methods into an MDO Framework for Optimal Redundancy in UAV Design

Robin Warren

Electrically-powered multirotor **Unmanned Aerial Vehicles (UAV)** are highly susceptible to rotor loss failures, which can result in catastrophic events in urban centers. Redundancy implementation can improve reliability, but heavily affects multirotor **UAV** performance. Hence, this research work aims at developing a design framework that may optimize multirotor **UAVs** for both performance and reliability. For this matter, a controllability assessment will be implemented in the design of multirotor **UAVs** to ensure fault-tolerant design.

An exploration of the design methodologies of multirotor **UAVs** demonstrates that only one includes redundancy analysis linked to controllability. The methodologies are classified into three major groups: empirical, analytical modeling and simulations, and analytical catalog-based. These classes are compared in a case study to demonstrate that analytical modeling and simulations are best suited for redundancy implementation due to their affinity with both innovation and reliability.

Since traditional controllability is not sufficient for multirotor **UAVs**, alternatives are evaluated. The **Degree of Controllability (DoC)** is chosen since it possesses recovery time requirement potential and the simple inclusion of disturbances. After modification for the application of the **DoC** to multirotor **UAVs**, it is implemented within the optimization framework of an analytical modeling and simulation design methodology, optimizing multirotor **UAVs** for both performance and reliability. The potential recovery time requirements of the **DoC** prove inconclusive because its value scales with time. Future works, through reference recovery regions, could forge toward aircraft-level controllability requirements. Nevertheless, including the **DoC** as a constraint yields fault-tolerant designs at a severe cost in computing time.

Acknowledgments

First and foremost, I must thank Dr. Liscouët for his dedicated support during this endeavor. He was a true guide for technical and professional inquiries and I can attest I have grown considerably while working at his side.

Second, I dedicate this research work to all the instructors who have supported me to this very point, without which this achievement would be unheard of. Whether it be the fifth-grade teacher or recent graduate professors, each has helped shape my knowledge and iron will to learn more. This achievement is just as yours as it is mine.

Next, I humbly thank all of my students and fellow teaching assistants, from which I have learned too much to grasp in mere words. Their eternal flame is one I relinquish to leave behind and one I aspire to see grow from either nearby or afar. I vouch to one day return to the whiteboard, if only to rekindle the ambers.

I send great thanks to my research lab mates, who have spiraled down the rabbit hole of multi-rotor control and performance with me. Research can be a lonesome pursuit, yet, I confirm that our research lab was always warmly lit with smiles, even in winter. Keep it that way in my absence.

Last but not least, I thank my parents and my sister for providing continual support, even when far from home. It is for you that I do this, and making you proud is my favorite hobby.

Contents

List of Figures	viii
List of Tables	x
Acronyms	xi
1 Introduction	1
1.1 Background	1
1.2 Problem Statement	3
1.2.1 How to Design for Competitive Performance?	3
1.2.2 How to Design for Heightened Reliability?	4
1.2.3 Design Challenges	5
1.3 Scope	5
1.4 Approach	5
1.5 Outline	6
2 Multirotor Design Methodologies	7
2.1 General Aviation Design Process	7
2.1.1 Optimization Framework	8
2.2 Overview of Design Methodologies	10
2.2.1 Empirical Methods	11
2.2.2 Analytical Methods	13
2.2.3 Extended Review	17

2.3	Case Studies	18
2.3.1	Selected Sizing Methodologies	18
2.3.2	Methodology	20
2.3.3	Results	23
2.4	Findings	26
3	Controllability for Reliability	28
3.1	Multicopter Dynamics Model	28
3.1.1	Moore-Penrose Pseudo-Inverse	30
3.2	Controllability	30
3.2.1	ACS	31
3.2.2	DoC	33
3.2.3	ACAI	33
3.2.4	Summary	34
3.3	Contribution	35
3.3.1	Multicopter DoC Methodology Development	35
3.3.2	DoC Computation and Results	41
3.3.3	DoC Implementation in Analytical Sizing Methodology	42
3.4	Case Studies	46
3.4.1	Methodology	46
3.4.2	Results	47
3.5	Findings	51
4	Conclusion	52
	Appendix A Design Methodologies N_2 Diagrams	54
	Appendix B Design Methodologies Input Analysis	58
	Appendix C Control Effectiveness Matrices	60
C.1	Quadrotor	61

C.2 Hexarotor	61
C.3 Octorotor	62
Appendix D DoC Configuration Analysis	63
Bibliography	65

List of Figures

Figure 1.1	DJI Phantom-4 Quadrotor UAV [1]	2
Figure 2.1	Aircraft Design Process [2]	8
Figure 2.2	Total Mass (W_o) with respect to the Ratio of Battery Mass to Total Mass (W_b/W_o) [3].	10
Figure 2.3	Classification of Multirotor UAV Design Methodologies	11
Figure 2.4	Case Study Methodology	20
Figure 2.5	Inputs and Design Parameters Required by Multirotor Design Methodologies	21
Figure 2.6	Traditional Multirotor Case Study	24
Figure 2.7	Heavy-Lift Multirotor Case Study	25
Figure 2.8	High-Endurance Multirotor Case Study	26
Figure 3.1	ACS Polytope [4]	32
Figure 3.2	ACS Polytope after Fault Injection (2D Plane) [4]	33
Figure 3.3	The Largest Enclosed Sphere within the ACS with Center g [5]	34
Figure 3.4	Control State Polytope and Recovery Region Illustrated in Three Dimen- sions [6]	38
Figure 3.5	The DoC of Multiple Different Multirotor Configurations	42
Figure 3.6	DoC for Different Recovery Times and Time Segments of Hexarotor	43
Figure 3.7	DoC Computing Times for Hexarotor Configuration	43
Figure 3.8	The Inter-Dependencies Between the Control Module and its Counterparts [7]	45
Figure 3.9	The Inputs Required for the Control Module [7]	45

Figure 3.10 The MTOW of Multirotor UAVs Optimized for Minimal Mass, Maximum DoC and Both Objective Functions	48
Figure 3.11 The MTOW of Redundant Multirotor UAVs with the ACAI and the DoC . . .	49
Figure 3.12 Hexarotor Mass of Traditional Design	50
Figure A.1 N_2 Diagram of the Empirical Methodology	55
Figure A.2 N_2 Diagram of the Analytical Modeling and Simulation Methodology . . .	56
Figure A.3 N_2 Diagram of the Analytical Catalog-Based Methodology	57
Figure C.1 Multirotor Configurations [8]	60
Figure D.1 DoC Configuration Analysis MTOW Results	64

List of Tables

Table 2.1	Case Study Design Requirements	22
Table 2.2	Design Parameters of the Traditional Case	23
Table 2.3	Design Parameters of the Heavy-Lift Case	24
Table 2.4	Design Parameters of the High-Endurance Case	25
Table 2.5	Design Methodologies State-of-the-art Findings	27
Table 3.1	Controllability Assessment Findings	35
Table 3.2	Controllability Case Study Requirements	46
Table 3.3	DoC and Computing Time of Effect of Controllability Case	47
Table 3.4	DoC and Computing Time of ACAI Comparison Case	49
Table 3.5	DoC of Design Features Exploration Case	50
Table B.1	Legend of Design Methodologies Input Analysis	58
Table B.2	Design Methodologies Input Analysis	59
Table D.1	Design Requirements of DoC Configuration Analysis	63
Table D.2	Rotor Diameter of DoC Configuration Analysis	63

Acronyms

ACAI Available Control Authority Index. ix, 31, 33–35, 41, 46–49, 51, 52

ACS Attainable Control Set. viii, 31–35, 51, 52

AMS Attainable Moment Set. 31, 32

BEMT Blade Element Momentum Theory. 12, 14, 15, 59

BLDC Brushless Direct Current. 14

BoM Bill of Materials. 15, 27, 59

CFD Computational Fluid Dynamics. 12, 13, 15

CG Center of Gravity. 15

DBS Database Management System. 17

DoC Degree of Controllability. iii, viii–x, 31, 33, 35–42, 44, 46–53, 60, 63, 64

ESC Electronic Speed Controller. 1, 11

FM Figure of Merit. 11, 13, 59

IMU Inertial Measurement Unit. 1

MDO Multidisciplinary Optimization. 9, 14, 19, 35, 44, 51, 52

MTOW Maximum Take-Off Weight. ix, 11, 12, 14–16, 19, 44, 47–50, 59, 64

T/W Thrust to Weight Ratio. [3](#), [14–16](#), [22–25](#), [46](#), [59](#), [63](#)

UAM Urban Air Mobility. [2](#)

UAV Unmanned Aerial Vehicle. [iii](#), [viii](#), [ix](#), [1–7](#), [9–14](#), [17–19](#), [28](#), [29](#), [31](#), [34](#), [35](#), [39](#), [40](#), [42](#), [44](#),
[48](#), [49](#), [51–54](#), [60](#)

VTOL Vertical Take-Off and Landing. [2](#)

Chapter 1

Introduction

Chapter 1 displays an overview of electric multirotor Unmanned Aerial Vehicles (UAV) and the perils associated with rotor failure while operating in urban centers. Such safety concerns will be explored by illustrating the current limitations in the design process of multirotor drones in terms of performance and reliability. The sections thereafter address the scope of work, the problem statement, the determined approach and finally an outline of the following chapters' contents.

1.1 Background

Fully electric multirotor UAVs, such as the DJI Phantom-4 shown in Figure 1.1 [1], generally have the following components: batteries, propulsors, avionics and an airframe. A propulsor is the assembly of a propeller, a motor and an Electronic Speed Controller (ESC), which regulates and controls the speed of the motor. Each propeller is generally optimized to spin either clockwise or counterclockwise, hence, they are generally unidirectional, and will be assumed as so for the purpose of this work. The avionics vary depending on the level of autonomy of the UAV, ranging from flight computers to Inertial Measurement Units (IMUs) and sensors. The airframe generally includes a main hub to load the avionics and batteries, arms depending on the multirotor configuration and landing gears.

For most traditional designs, all rotors are part of the same plane with the exception of the trirotor, which requires the rotors to be tilted for yaw control. General configurations include trirotors,



Figure 1.1: DJI Phantom-4 Quadrotor UAV [1]

quadrotors, hexarotors and octorotors, but may vary due to the arrangement of lifting devices and the addition of coaxial propellers. Such coaxial installations induce negligible losses in efficiency compared to the benefits of increasing the lift potential of the aircraft by 40% [9]. An array of multirotor configurations are illustrated in Figure C.1. Indeed, the placement and size of rotors on multirotor UAVs is an ongoing research field [10], in eternal search of the most optimal arrangement of rotors for specific sizing scenarios.

Multirotor UAVs have seen seamless progress in recent years, in parallel with the development of Urban Air Mobility (UAM). In fact, multiple major industries including Google, Amazon, UPS and DHL [11] are currently developing their own multirotor products. Although the economic feasibility of passenger-carrying UAMs is ongoing research [12], its cargo-transporting counterpart shows much promise [13, 14]. Indeed, in the later years, their potential applications have only grown: spanning photography, search and rescue, firefighting, agriculture, construction and the transport of goods [15]. Much of these applications are required in urban centers, where Vertical Take-Off and Landing (VTOL) capabilities are a requirement. Nevertheless, such applications require heightened safety requirements considering they are expected to operate over the line of sight in densely populated areas. Numerous dangerous cases of the use of multirotor UAVs in cities have been reported, including interference with global aviation, harm to human lives and damage to property [16].

Hence, multirotor UAVs should become more reliable to be implemented in urban sectors. Although covered in greater detail in Chapter 2, initial research demonstrates that reliability is not effectively applied during the design process of multirotor UAVs [17]. Thus, the reliability aspects of such sizing methodologies could be increased through the use of redundancy analysis, which is state-of-the-art in general aviation [18]. However, in the case of multirotor UAVs, the application of redundancies is a significant challenge. Redundancies may affect the performance of the overall product in dire ways, such as resulting in increases in mass of up to 82.5% [17].

Thus, the present research aims at determining a pathway to optimize multirotor UAVs for both performance and reliability.

1.2 Problem Statement

The following section will outline the main issues within the sizing of multirotor UAVs to achieve both heightened reliability and competitive performance. Then, the antagonistic nature of their integration is explored further to determine the path to a solution.

1.2.1 How to Design for Competitive Performance?

The performance of electrically powered UAVs is heavily dependent on multiple factors, one of which is weight. The weight of any aircraft is directly connected to its flight performance, however, it is specifically an issue for electric multirotor systems using current battery technologies. Indeed, the energy density of batteries is the main limitation to their flight time and autonomy, which may cause the divergence of certain design solutions. Any additive mass during the design process will result in a greater energy demand, which then leads to a heavier battery in a snowball effect fashion. Considering weight is critical for any aircraft, this cycle may force the battery mass to expand until the aircraft itself becomes too heavy to fly.

Similarly, the multirotor's propulsors equally affect its performance. More specifically, these components define the maneuverability of the product, often quantified as a Thrust to Weight Ratio (T/W). This demonstrates the range of thrust the multirotor can provide, which may then relate to its flight speed, climb acceleration and maximum altitude. This is dependent on the multirotor UAV

configuration, which affects the total number of propulsors they may possess. The thrust generated by a rotor is shown in Equation (1) [19], which itself is a function of air density (ρ) ($\frac{kg}{m^3}$), rotor area (A) (m^2) and the velocity induced by the rotor (v_i) ($\frac{m}{s}$). A larger area covered by the rotating blades of a rotor results in a higher thrust. Hence, the maximal thrust is limited by the configuration of the propulsors and the maximal requirement for the size of the multirotor: the maximum attainable disk area.

$$T = \dot{m}w = 2\rho Av_i^2 \quad (1)$$

1.2.2 How to Design for Heightened Reliability?

The potential failures of UAVs within urban centers are plentiful [16], to cover all of them is a monumental task. This work focuses on the loss of control failure, which is particularly critical for multirotor [20]. Indeed, multiple factors may lead to a loss of control including propeller failure, adverse flying conditions, changes to flying quality, loss of control effectiveness or combinations of these [20]. This work will focus on the failure of a propulsor, which, depending on the multirotor configuration, will affect the controllability of the system differently. Failure of propulsors may be related to an impact, mechanical failure, power management system failure, or else. This could lead to a total loss of control, which would be catastrophic in urban centers. And, as general aviation states, such catastrophic failures should have a probability of occurrence lower than 10^{-7} [21] per flight hour. Moreover, these standards state that “no single failure shall lead to a catastrophic event” [22]. In such cases, catastrophic events are classified as leading to the loss of human life.

The sensibility of multirotor to loss of control and propulsor failure depends on their configuration and sizing. Normally, coaxial and additional rotors aid in such endeavors. However, it depends on the overall arrangement of the rotors and which are lost, since they each play their role in the fully-fledged control allocation of the aircraft. One common method to increase reliability is the inclusion of redundancies [18] to achieve fault-tolerant designs. This may yet affect dramatically the performance and competitiveness of a multirotor UAVs [17], which leads us to the problem at hand.

1.2.3 Design Challenges

The integration of both performance and reliability is a challenge, as they are antagonistic in a variety of ways. As stated previously, the weight of multirotor UAVs is critical. Battery technologies amplify any addition to the mass and severely hinder its performance. Conversely, the most appropriate method to increase reliability is redundancy, which often dramatically increases the mass. This is additionally an issue for attainable disk area, as the number of rotors may only be increased up to a certain margin. Moreover, reliability can be increased through conservative designs, while competitive performance is the result of innovation.

Considering their averse nature, their implementation could lead to unmet requirements and or divergent solutions, even when nested within an optimization framework. The path to a solution lies in implementing redundancy analysis into the design process while taking into account its effect on the product's energy efficiency and mass budget.

1.3 Scope

The present work aims at implementing heightened reliability for rotor loss failures into the design and sizing process of fully electric multirotor UAVs in order to optimize the aircraft for both competitive performance via high-fidelity sizing compatible with redundancy analysis and enhanced reliability through a controllability assessment implementation.

1.4 Approach

The approach will be as follows:

- Review the state-of-the-art for multirotor UAV design and sizing methodologies and determine their ability to host a redundancy analysis through case studies
- Review the controllability of multirotor and determine an assessment method that is the best fit for implementation within a design methodology

- Apply effectively a propulsor redundancy analysis based on controllability within the design process of multirotor UAVs to ensure the definition of fault-tolerant designs

1.5 Outline

This research work begins with a general introduction to multirotor UAVs and the design challenges associated with loss of control failures in urban centers. The problem is stated by focusing on the antagonistic nature of both performance and reliability requirements. Chapter 2, after exploring the general aviation design process and the optimization framework of a design problem, reviews the state-of-the-art of multirotor UAVs and classifies them based on their ability to host a redundancy analysis. Then, a case study will evaluate the best fit for redundancy implementation. Chapter 3 evaluates the dynamics model of multirotor UAVs and controllability before reviewing the available controllability assessments, which may grant redundancy to loss of control failures. A chosen assessment is then implemented within a design methodology to optimize for both performance and reliability within a case study. Chapter 4 concludes this work with the overall findings and evaluates the potential future works.

Chapter 2

Multicopter Design Methodologies

The first step in the implementation of reliability in the design process of multicopter UAVs is to review the state-of-the-art sizing such products. In this section, general aviation design will be presented to aid in the classification of the state-of-the-art. Then, the current design methodologies of multicopter UAVs will be classified and explored to define their affinity with reliability and redundancy. Three examples of methodologies will be compared in case studies to evaluate their capability to implement redundancy analysis. To conclude the section, the overall findings are provided.

2.1 General Aviation Design Process

The design of complex systems, such as aircraft, is divided into three main phases: conceptual, preliminary and detailed design [22]. Raymer [2] and Roskam [23] provide extensive pathways and methods to design aircraft depending on their design phase. The conceptual design phase is where the initial sizing is determined. The preliminary design phase shrinks potential solutions further and, finally, the detailed design is where all aspects of a product are known and sized [2]. The design resources required with each design phase increase. The aircraft design process is illustrated in Figure 2.1.

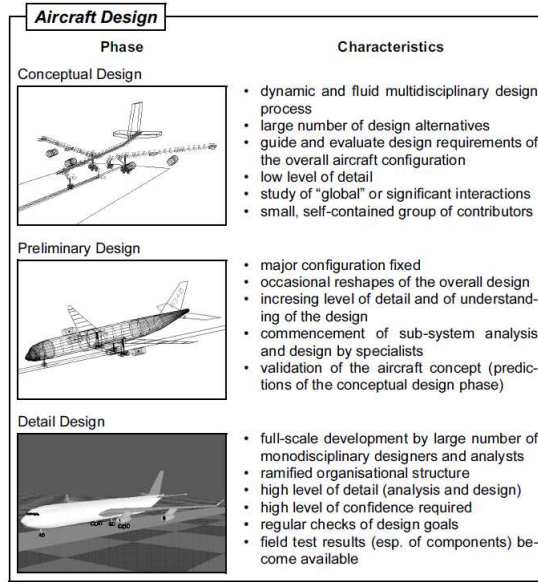


Figure 2.1: Aircraft Design Process [2]

To accurately classify the sizing methodologies of the state-of-the-art, they each should be assigned to a respective design phase since they have different requirements in terms of fidelity, validation and design space refinement. As an example, a conceptual design methodology should have lesser inputs than a detailed methodology. Such classification will aid in determining which design phase is the best fit for the implementation of redundancy analysis.

2.1.1 Optimization Framework

Design challenges are often formulated as optimization problems. Methodologies will be compared with respect to this framework to illustrate their differences, which largely occur within the details, including constraints, objective functions and design variables. As such, the framework of such optimization is presented below, along with a few examples for multirotor design.

Given that,

$$x \in \mathbf{R}^v$$

And,

$x = (x_1, x_2, \dots, x_v)$ in the solution space X

*Find x^**

Such that it minimizes $F(x^)$*

Subject to

$$g_n(x) \leq 0, h_m(x) = 1 \text{ for } n, = 1 \text{ to } p$$

Where,

- x is the design variable vector, which contains v different design variables.
- x^* is the optimal design variable vector.
- $F(x)$ is either the objective function or a vector of multiple objective functions.
- $g_n(x)$ and $h_m(x)$ are respectively inequality and equality constraints.

Mass minimization is often the objective function for multirotor UAVs, as it is directly linked to their performance. However, other cases may include energy minimization or range maximization. Design variables may include propeller diameter or battery mass, as they may be optimized according to different objective functions. Multiple objective functions may also be included within the same optimization framework in a Pareto front [24], which assigns respective importance to multiple objective functions within the same framework. Moreover, the optimization of such products may be Multidisciplinary Optimization (MDO), which includes multiple different disciplines within the same framework, including aerodynamics, structures, electrical, etc. In such cases, the design variables are numerous, as they tackle a wide variety of characteristics of multirotor UAVs.

The nuance within the classification of the methodologies lies in the various different constraints. As an example, a conceptual design methodology [3] imposes an equality constraint on

the battery mass of multirotor UAVs. As illustrated in Figure 2.2, a trend is defined based on the total mass W_o and the battery mass fraction $\frac{W_b}{W_o}$, which refers to the allocated portion of the total mass which the battery occupies within the mass budget. This trend of commercial multirotor UAVs is used to define the total mass of the battery during the design process as a constraint, shown in Equation (2) [3].

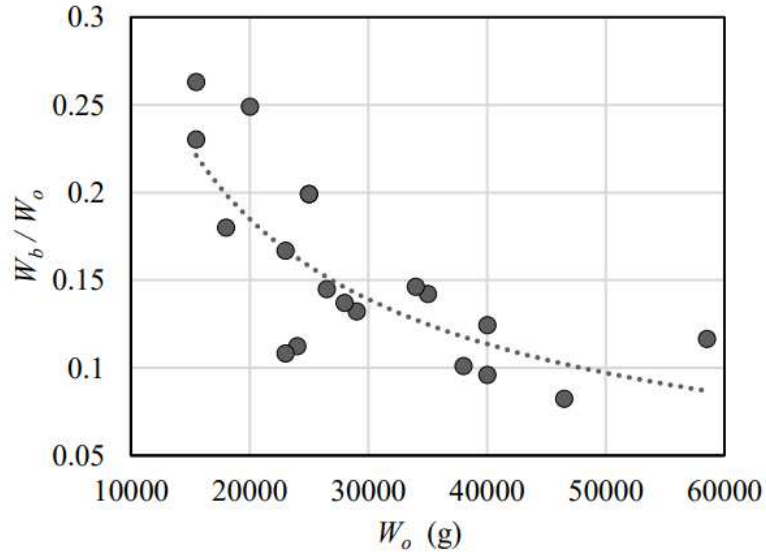


Figure 2.2: Total Mass (W_o) with respect to the Ratio of Battery Mass to Total Mass (W_b/W_o) [3].

$$\frac{W_b}{W_o} = 195.27W_o^{-0.703} \quad (2)$$

2.2 Overview of Design Methodologies

This section will outline the state-of-the-art for multirotor design methodologies. They will be classified into two main different groups: empirical and analytical as a result of the review. This classification is an expansion of previous works [25]. Analytical methods will be separated into two sub-categories: methodologies which use modeling and simulation and methodologies which are based on off-the-shelf catalogs. Some design processes will make use of both empirical and analytical tools, classified as hybrids. The methodologies will be shown in the order displayed

by Figure 2.3. An additional section is dedicated to other references not specifically outlining a methodology but connected to the subject matter.

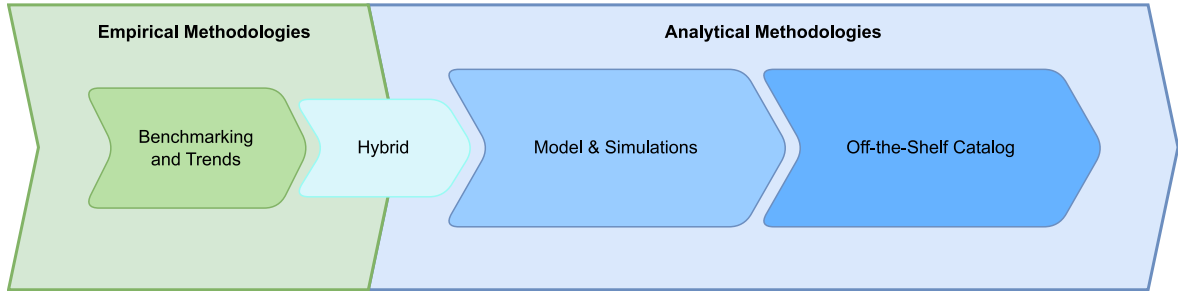


Figure 2.3: Classification of Multirotor UAV Design Methodologies

2.2.1 Empirical Methods

Empirical methodologies heavily apply regression trends and commercial data analysis to design products, estimating the mass of each component based on previous market trends and benchmarking. Such methods should be used during conceptual design, as they require few inputs to function. The empirical methods will be shown in chronological order.

Gatti [26] defines empirical regression trends for each of the components of the multirotor, whether it be the motors, battery, ESCs or even the structure. Mass fractions for each of the components restrict the sizing process, which iterates its hover power computations until the endurance requirements are met. The data used in most of the trends inherent to this methodology is limited to multirotor UAVs with a Maximum Take-Off Weight (MTOW) lower than 20 kg, which may lead to divergence in some sizing cases outside that range. Moreover, these trends are restricted to conventional designs without redundancies.

Ong [3] manages mass fraction trends as well for coaxial multirotor designs. The focus of this methodology is to size heavy-lift drones and its main contribution is the inclusion of the aerodynamic effects of coaxial propellers. The propulsion requirements are extensive and are based on rotor size, configuration and their estimated Figure of Merit (FM), which quantifies the losses in mechanical and aerodynamic efficiency of propellers. This methodology also makes use of Raymer trade studies [2] to iterate.

The scope of empirical methodologies does not merge with reliability needs, considering the overall maturity of the product. During this phase, architectures and components specifications are unknown and hence, reliability analysis is difficult to implement. Moreover, the reliance on market trends hinders such reliability implementations as they are not effectively integrated into current multirotor designs. Empirical methodologies are good performance estimation tools with minimal inputs to assess the feasibility of design solutions in early sizing. However, they do not refine the design space enough to warrant a reliability analysis.

Hybrid Methods

The methodologies in this section make use of both empirical tools such as regression trends and analytical tools such as modeling. Most consider analytical tools to compute power conditions or aerodynamic parameters. They will be shown in chronological order.

Bohorquez [27] focuses on the development of an optimization framework to properly define propeller performance in hover conditions. Then, the Blade Element Momentum Theory (BEMT) analysis, which computes the local aerodynamic forces on segments of rotor blades, is coupled with an airfoil database to obtain additional parameters. The database results are empirically interpolated to determine specific local aerodynamic parameters.

Winslow [28] defines empirical trends for each of the components of a quadrotor except the propellers, which use BEMT analysis. The precision of this analysis was validated against high-fidelity Computational Fluid Dynamics (CFD) airfoil results. The validation of this method only covers micro air vehicles (MTOW lower than 1kg), which may influence its range of applications for delivery multirotor UAVs.

Vu [29] describes the electric propulsion model of a quadrotor with empirical regression models, aerodynamic analytical consideration and global mission requirements. Although it may be considered empirical, the in-depth analysis of propeller performance based on advanced helicopter aerodynamics [19] secures its position as a hybrid methodology.

Bauersfeld [30] builds a hybrid methodology containing both empirical regression models and BEMT analysis for propeller blade performance. The propeller model was validated against off-the-shelf

propulsor combinations, similarly to the overall sizing process, which was validated with the manufacture and testing of a prototype.

Hybrid methodologies have similar downsides and upsides to empirical methodologies based on their reliance on trends. However, their use of analytical models and tools grants them further fidelity. None of the hybrid methods tackle reliability and redundancy.

2.2.2 Analytical Methods

Analytical methodologies employ modeling with physical equations, simulations and off-the-shelf catalogs to size multirotor UAVs. The scope of analytical methods can refer to both models of individual systems or the entire multirotor. Multiple analytical methods referring to different systems can be assembled into larger sizing processes.

Modelling and Simulation Methods

The methods in this section make use of models or simulation tools to define multirotor UAVs. Models, as examples, cover the propulsion system, the aerodynamics of propellers, the airframe geometry, etc. Simulations, on the other hand, make use of more detailed tools such as CFD. These procedures require more inputs and shrink the array of potential solutions more than empirical methodologies, hence, they are employed in the preliminary design phase. The methods will be shown in order from most modeling-focused to most simulation-based.

De Angelis [31] defines the power required at hover and an FM characterization analytically through the development of a physical model of the propeller. The aerodynamic characteristics of the propellers can be determined analytically instead of experimentally. The model is then combined in a framework of physical equations to simulate power draw, and flight time to establish its optimal performance.

Quan [5] defines in detail the design requirements which shape multirotor UAVs. It covers the variety of components required for sizing, aerodynamic effects and control considerations. Rather than developing an over-arching methodology, this work demonstrates multiple different approaches for various systems of design with a strong focus on hardware selection.

Ampatis [32] employs analytical models for each of the components and optimizes for two

different objective functions: vehicle total energy or vehicle diameter. All models are developed to compute component size as well as performance and allow for the overall product area to be optimized. A domain for each component size can equally be determined.

Bershadsky [33] presents an optimization framework rooted in a flight time calculator which includes the sensitivity analysis of various parameters including **MTOW**, battery capacity, propeller diameter and more. Although its multirotor functions are observed for the purpose of this paper, the tool may also be used for winged designs. The flight performance data is determined from a **BEMT** analysis, which may lead to uncertainties due to the assumed airfoil within the methodology.

Gadekar [34] demonstrates an analytical methodology for a fuel-powered multirotor with variable pitch propellers. The change to variable pitch affects the control of the aircraft significantly while not using electrical power increases its performance.

Oh [35] defines a sizing methodology for multirotor **UAVs** with an **MTOW** lower than 25 kg. Through aerodynamic, structural, electrical and performance models, the optimization algorithm sizes a multirotor as per specific mission profile requirements such as climb acceleration or cruise time.

Szafranski [36] develops a model for the propulsion unit of a multirotor. This model encompasses an ESC, an electric Brushless Direct Current (**BLDC**) motor and a propeller. Although this work focuses on a single system, rigid frame aerodynamic considerations are included to ease pairing with other methodologies and hence size a full multirotor.

Mascarello [37] builds a multirotor ballistic model to ensure that the sized product may not cause harm in the event of any failure. This work's focus is enhancing the inherent safety of the product's structure, other systems are not considered in depth. Multiple hazards and accidents caused by **UAVs** are equally reported.

Delbecq [7] makes use of scaling laws, physical models and **MDO** to develop an optimization framework including constraints imposed by each of the multirotor components. Other constraints include mission profile requirements, **T/W** and various sizing case scenarios. Multiple objectives are available including minimizing the **MTOW**, maximizing the range, maximizing the endurance, and so on. This framework is particularly permeable to the addition of other optimization modules, including the addition of reliability evaluation [8] through controllability analysis. Such means of

attaining reliability will be tackled in greater detail in Chapter 3.

Ye [38] optimizes quadcopter propulsion systems in forward flight through BEMT analysis and CFD. Models within are either empirical, for the motor, rotor and battery mass, or analytical, for the fuselage and rotor aerodynamics. Nevertheless, the use of high-fidelity CFD increases the computation time significantly.

Phang [39] discusses the systematic design of micro quadrotors. This methodology harnesses a 3D virtual environment for sizing, involving MSC Patran, Nastran and Solidworks. Nevertheless, this method is for quadrotors with an MTOW lower than 3 grams.

As observed, analytical methodologies are more varied than empirical processes. Most require more inputs than their empirical counterparts and refine the design space further. They may calculate the requirements for one of the systems or the multicopter as a whole and could be combined in any manner of ways. Some of the outlined methodologies do tackle reliability, safety or control needs [5, 8, 34, 37]. This demonstrates that reliability analysis may be performed during the preliminary design phase.

Catalog-based Methods

Catalog-based methodologies apply optimization to determine the best components for specific sizing requirements based on off-the-shelf databases of parts. As a result, the output of these methods is a complete Bill of Materials (BoM) ready for assembly. As such, they often require more parameters and define the optimal solution within the design space, considering they must be paired with databases of components and their performance data. They are thus tailored for the detailed design. The catalog-based analytical methods will be shown in chronological order.

Ng [40] optimizes the MTOW of a quadcopter through a genetic algorithm, making use of constraints such as the distance between the propellers, the Center of Gravity (CG) location, the T/W and the balancing of various aerodynamic moments on the structure. This methodology was also validated through a case study including the performance of off-the-shelf components.

Magnussen [41] establishes an optimization framework to determine the optimal combination of components from a discrete set of data through a mixed-integer programming methodology.

Arellano-Quintana [42] defines an optimization framework for two different objectives: maximum T/W and maximum flight time. The use of a genetic algorithm links the methodology with off-the-shelf products and implements a component selection.

Du [43] combines geometrical optimization and simulation into a user-friendly computerized interface. A variety of different structures can be developed within the interface and they can be readily optimized before their flight performance and control are simulated. Hence, iterations with this tool lead directly to fabrication as most items part of its catalog are readily available.

Biczyski [44] defines an optimization framework to define motor and propeller selection based on an analytical model of batteries including flight time estimation. The voltage diminution of the battery during operation is acutely captured within the analytical model. The optimization permits to tailor the problem statement to specific operational requirements.

Ayaz [45] develops a multi-objective optimization methodology using a genetic algorithm to define multicopter sizing based on off-the-shelf components. Hence, the multicopter can be optimized for three different roles, which are $MTOW$, total flight time and overall cost.

Dai [46, 47] develops an optimization framework linked to component databases. Each component is associated with performance parameters, including compatibility with other components, such as the efficiency as a result of a motor and propeller pair. Moreover, each component possesses safety parameters which are part of the optimization. Nevertheless, the optimization's scope is at the system level, and not the multicopter level. The methodology is automated as an online tool known as Flyeval [48].

Renkert [49] builds a hybrid optimization framework through the parameterization of design drivers and the use of both search and genetic algorithms. The optimization is achieved through the conversion of the discrete domain variables to a continuous domain to use gradient-based methods. Cost data is available, providing interesting statistics on the overall cost of maximizing energy efficiency.

Catalog-based methodologies go further than modeling and simulation processes and completely size a product. Considering the level of maturity of the product, reliability analysis based on architectures would be possible since component specifications are known. Nevertheless, only

one such methodology [46, 47] mentions the inclusion of reliability, while one other mentions control [43]. Moreover, the reliance of the methodologies on components skews the available design space, which becomes discrete instead of continuous in the case of empirical or other analytical methodologies. Hence, an optimal design that would require non-existent parts is disregarded, even though these components could be designed for such performance. Innovative designs with competitive performance are then harder to obtain since there is no ability to create new parts for specific ventures.

2.2.3 Extended Review

This section outlines additional work pertaining to the subject matter of sizing of multirotor UAVs while not containing a new sizing methodology. The following sources rather demonstrate issues within the sizing or paths toward improvement.

Achtelik [50] encompasses the implications of increasing the number of rotors for multirotor UAVs, including redundancy. Although not a full methodology, the performance evaluation of different design configurations demonstrates the feasibility of redundancy implementation in multirotor designs.

Basset [51] outlines the sizing methodologies of rotorcraft used at Onera, a French aerospace research center. Although each of the methods are not covered in depth, their main inputs and outputs are displayed along with their implementation in the aircraft design process. The advantages of multi-disciplinary optimization are equally demonstrated, outlining the modularity of such frameworks and the ease of implementation of new modules, which could consider reliability.

Rana [52] explains the use of a Database Management System (DBS) of methodologies for aircraft design. Different other sizing methodologies could be building blocks the software would use to define the best potential sizing methodologies appropriate for specific design requirements. Instead of building a database of components such as the catalog-based methods shown prior, a catalog of methodologies could be utilized to define which methods are optimal for the user's specific requirements at a specific design phase. This finding illustrates the need to classify design methodologies as they may be combined together to obtain more effective means of sizing multirotor UAVs.

2.3 Case Studies

To analyze further the difference between the three main classes of methodologies outlined in section 2.2, a case study is developed. Its goal is to determine which type of methodology is best for implementing redundant features while preserving competitive performance.

2.3.1 Selected Sizing Methodologies

The three methodologies chosen for the case studies are:

- The empirical methodology defined by Ong et al. [3].
- The analytical modeling methodology defined by Delbecq et al. [7].
- The analytical catalog-based methodology defined by Dai et al. [46, 47].

The methodologies were chosen with regard to their availability, ease of use and potential for reliability analysis implementation. Each methodology will be detailed further in the following section, while detailed N_2 diagrams [53] for each are shown in Appendix A.

Empirical

The methodology defined by Ong et al. [3] is chosen since it is the most permeable to change in its inputs and can be applied to a greater range of multirotor UAVs while compared to Gatti [26], which is tailored to lightweight drones. Figure A.1 illustrates the methodology in an N_2 diagram [53].

The main inputs of this methodology are the payload mass, the number of rotors, the rotor area and the required flight time. Most models within the methodology are empirical, hence based on regression trends. The available flight time is then evaluated with Raymer trade studies [2] to define iteration parameters and correct the battery mass fraction until convergence is met.

This methodology does not use a traditional optimization framework, hence, its results should not be treated as optimal. This tool rather defines a useful estimate of performance parameters for early conceptual design.

Furthermore, this methodology does not address reliability considering the early phase of the design it should be applied at. Its application of market trends does not encourage the implementation of heightened reliability considering its regression trends are based on currently available components, which lack reliability features. The use of this methodology within the case studies could demonstrate if heightened reliability will influence the accuracy of early performance estimates of multirotor UAVs.

Analytical Modeling and Simulation

The methodology introduced by Delbecq et al. [7] is chosen since further studies consider reliability implementation [8]. Its optimization framework lends itself to the implementation of alternate modules due to its use of MDO-based coding, OpenMDAO [54]. The methodology is illustrated in Figure A.2.

The main inputs of this methodology are the payload mass, the number of propellers, the acceleration at take-off, the flight time, the number of arms and the number of rotors per arm. Due to its implementation in object-oriented coding, most of the parameters affecting the analytical models can be readily modified with ease. This methodology uses MDO to define a product. Furthermore, multiple objective functions can be utilized including minimizing the MTOW, maximizing the range or maximizing the endurance. Mission definition is quite extensive, including the definition of emergency diversions, range and expected cruise speed.

Its optimization framework is particularly modular: the addition of new models and new constraints could lead to the implementation of reliability into the design process, as shown by Liscouet et al. [8]. To compare the methodologies on equal footing, this reliability implementation will be employed for this case study along the non-redundant variant [7]. These methodologies will demonstrate the effect of redundancy implementation at the preliminary design level.

Analytical Catalog-Based

The methodology outlined by Dai et al. [46, 47] since it is publicly available online, known as Flyeval [48]. It is illustrated in Figure A.3.

The main inputs of this methodology are the payload mass, the number of rotors, the flight time,

the flight altitude, a specific sizing case scenario (hover, cruise, heavy-lift, etc.), flight altitude and the type of battery technology used. From these values, the sizing process determines a range of different solutions with different components and varying performance.

As previously explored, optimization frameworks provide modularity which may lead to the implementation of reliability. The off-the-shelf database is indeed linked to safety requirements, however, these are not available from the user interface. Moreover, as the databases are related to the currently available components, innovation may not be at the forefront since the optimization is discrete in nature. For the following case study, this sizing process will be applied to define the effect of redundancies at the detailed design level.

2.3.2 Methodology

The three methodologies will be compared with respect to the same design requirements. Three different cases will be obtained: traditional, heavy-lift and high-endurance. These will then be compared to redundant counterparts. This process is illustrated in Figure 2.4.

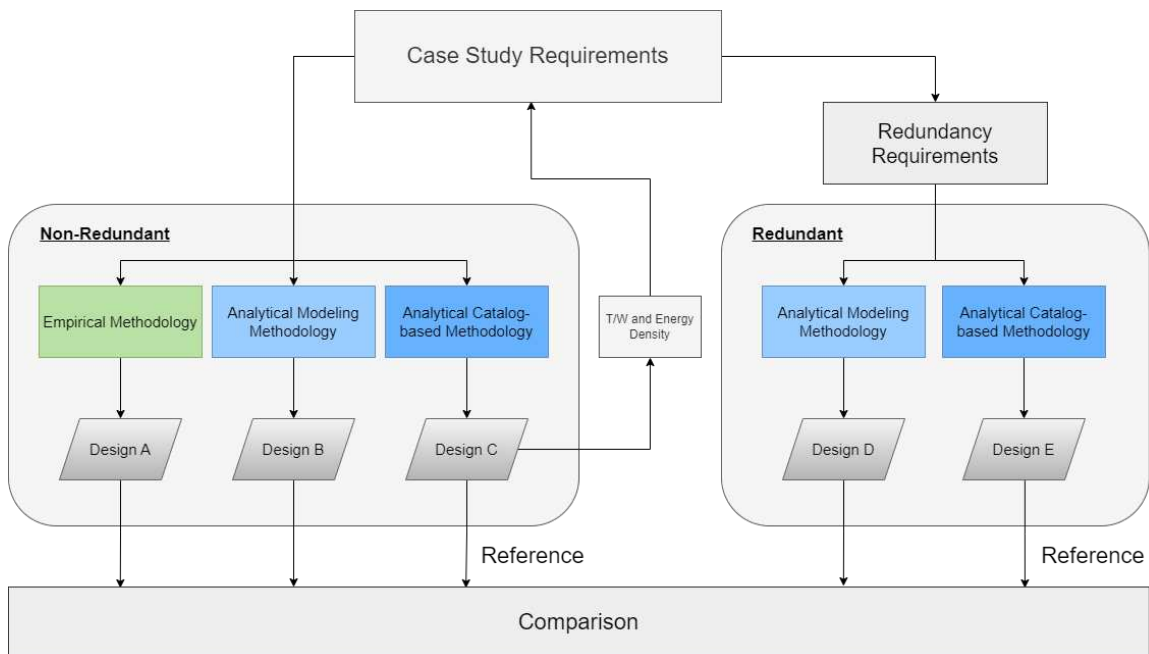


Figure 2.4: Case Study Methodology

A normalization effort must take place, to warrant a fair comparison between all methodologies

respectively. Indeed, the amount of inputs and parameters for the design methodologies follows a trend similar to the one shown in Figure 2.5, stating that methodologies in later design phases will require more inputs and design parameters. The result will as a consequence have greater design fidelity.

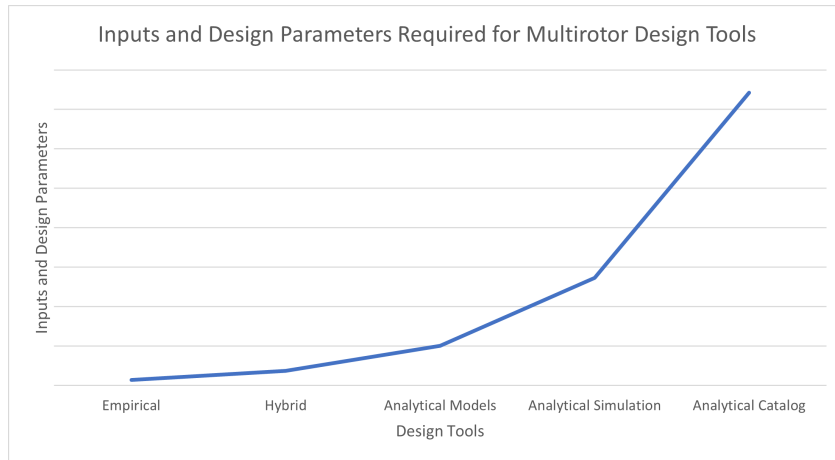


Figure 2.5: Inputs and Design Parameters Required by Multirotor Design Methodologies

First and foremost, since the catalog-based methodology does not allow tampering with energy density, it will always output the battery technology which is the best fit for the requirements. Hence, its resulting energy density will be used for the empirical and analytical modeling and simulation methodologies.

Second, the propeller diameter illustrates the disparity among the sizing methods. Primarily, the empirical requires the propeller diameter as an input while the other two determine the optimal diameter during the sizing process. Hence, a propeller diameter range will be set during the case study for all methodologies. As will be observed, the empirical methodology will always maximize the diameter of its propellers to maximize available disk area.

Third, the requirement for flight time is applied differently for certain methodologies. For the empirical and modeling methodologies, if the requirement is not met, the process will not converge to a solution. On the other hand, the catalog-based method, due to its discrete design space, displays the solution closest to the requirement, which may induce differences. To mitigate this, considering the catalog-based methodology determines multiple potential solutions, its result with the flight time

closest to the requirement will be chosen each time.

Fourth, the T/W cannot be set for the catalog-based methodology, as it is a design variable depending on the mission type. Hence, the T/W requirements for both the empirical and analytical modeling methods will be the same as the results from the catalog-based methodology.

Finally, in the case of the implementation of coaxial rotors, the effect of coaxial performance should be maintained constant through all methodologies. Hence, the losses in efficiency will be maintained at 20% [9, 19]. To illustrate the scale of the normalization, Table B.2 in the Appendix B displays all the inputs and parameters inherent to each methodology.

Case Study Requirements

The design requirements for all the cases are shown in Table 2.1.

Table 2.1: Case Study Design Requirements

Design Requirements	Traditional	Heavy-Lift	High-Endurance
Payload (kg)	2.5	10	2.5
Number of Rotors	4	8	8
Rotor Diameter Range (m)	0.2 to 0.8	0.2 to 0.8	0.2 to 0.45
Coaxial	No	Yes	Yes
Flight Time (min)	10	20	30
Flight Altitude (m)	100	50	100

As seen in the Table B.2, these inputs are common for all methodologies.

Redundant Designs

For each of these cases, the redundant sizings will be obtained as a derivation of their respective methodologies. In the case of the analytical modeling and simulation methodology, the processes shown by Liscouet et al. [8] will be followed, which include additional coefficients for motor mass estimation and emergency diversion estimates.

As of the analytical catalog-based method, the process shall be as outlined by Nazarudeen et al. [17]. A reliable reference will be simulated through additive payload within the catalog-based methodology, while validating that the obtained answer still meets the initial design requirements,

displayed in Table 2.1. For this purpose, the battery will be doubled to attain full battery management system redundancy. The frame mass will be increased by 50% to contain additive redundant components. Designs that are not coaxial, such as the traditional case, will become coaxial to prevent loss of control failure. As such, the resulting reference may not be the optimal solution to the design problem. Nevertheless, this manner of sizing is an estimation of the potential of a reliable sizing methodology for multirotor, which currently is not present in the state-of-the-art.

2.3.3 Results

The following section will outline and discuss the results of the case study.

Traditional Case

In the traditional case shown in Figure 2.6, the effects of adding coaxial rotors can be observed in the disparity between the redundant results and their counterparts. Moreover, it is shown that for traditional designs, the empirical methodology provides a good estimate of detailed design results from the catalog-based method. The propeller diameter and T/W of each of the designs are shown in Table 2.2, showing a steep decline in T/W from the redundant catalog-based design. Although the modeling and simulation method displays affinity with redundancy, it cannot yet match the results of the redundant catalog-based estimate.

Table 2.2: Design Parameters of the Traditional Case

Methodology	Propeller Diameter	T/W
Empirical	0.8 m	2.25
Modeling	0.656 m	2.25
Catalog-Based	0.6 m	2.25
Redundant Modeling	0.5 m	2.25
Redundant Catalog-Based	0.6 m	1.5

Heavy-Lift Case

In this case, shown in Figure 2.7, all multirotor designs are coaxial. Nevertheless, the high payload requirements pushed some methodologies to severely increase their propeller diameter, as

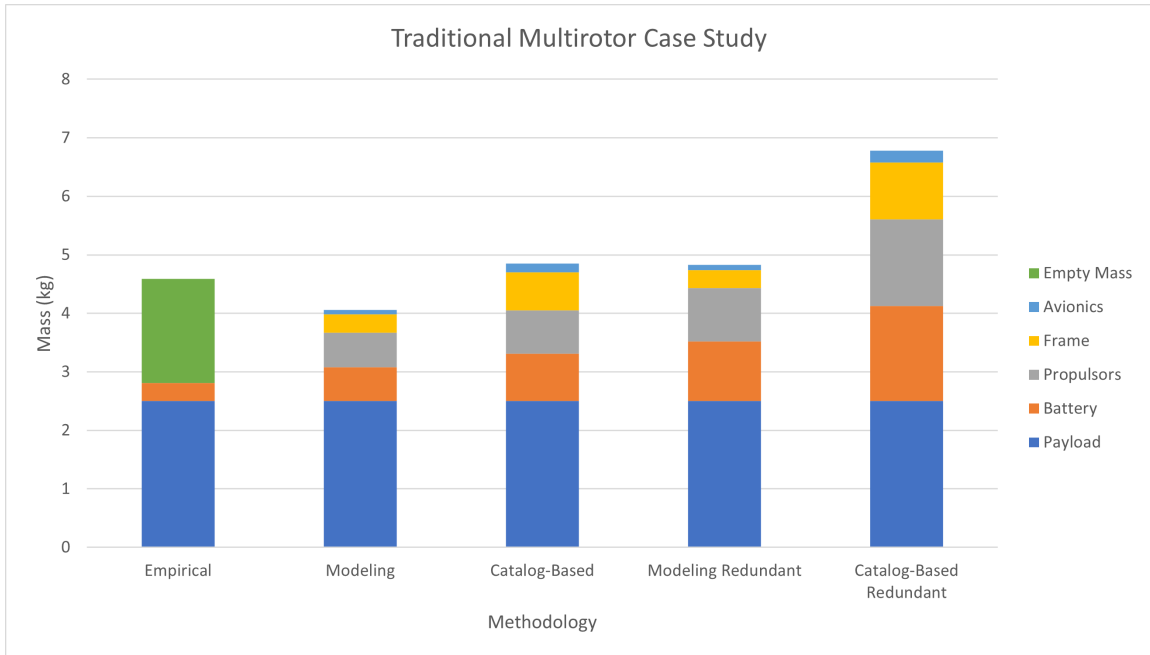


Figure 2.6: Traditional Multirotor Case Study

shown in Table 2.3. Since the empirical methodology always maximizes the propeller diameter, it may be overly optimistic in its battery estimations. The frame and propulsor computations of the analytical modeling and simulation methodology are also considered optimistic when compared to the catalog-based non-redundant and redundant results. However, the redundant version of the modeling and simulation design process achieves at 12.5% difference with the redundant catalog-based design, an offset mostly rooted in the frame mass disparity.

Table 2.3: Design Parameters of the Heavy-Lift Case

Methodology	Propeller Diameter	T/W
Empirical	0.8 m	1.95
Modeling	0.75 m	1.95
Catalog-Based	0.71 m	1.95
Redundant Modeling	0.7 m	1.95
Redundant Catalog-Based	0.71 m	1.25

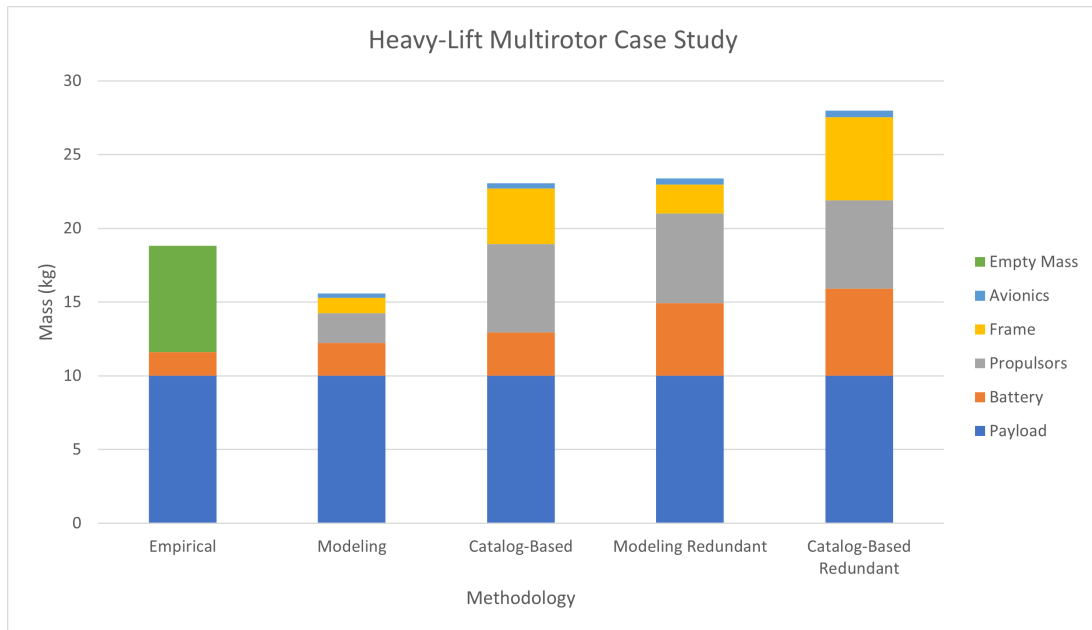


Figure 2.7: Heavy-Lift Multirotor Case Study

High Endurance Case

It should be noted that for this case, shown in Figure 2.8, the redundant methodologies cannot provide convergent designs. Hence, the addition of redundancies along the design process has led to divergence, even if the design could appear as previously plausible in earlier design phases. Moreover, this case shows a steep increase in mass from the empirical and modeling and simulation methods to the catalog-based results. As shown in Table 2.4, the T/W is similar for all methods, while the modeling and simulation method has a slightly smaller propeller.

Table 2.4: Design Parameters of the High-Endurance Case

Methodology	Propeller Diameter	T/W
Empirical	0.45 m	1.58
Modeling	0.316 m	1.58
Catalog-Based	0.43 m	1.58

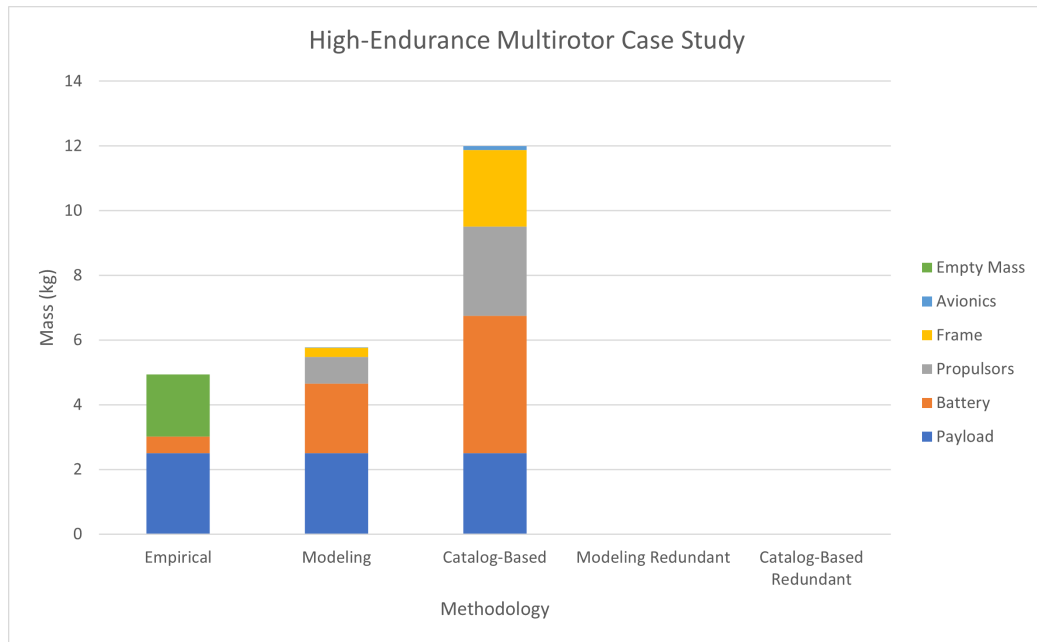


Figure 2.8: High-Endurance Multirotor Case Study

2.4 Findings

The review of the state-of-the-art sizing methodologies outlines the challenges associated with the implementation of reliability in the design process. Empirical methodologies, as seen in the case studies, are often optimistic in their estimations and far from redundant design expectations. These methods are best for early conceptual design, as they are tailored to conventional designs without reliability considerations.

Analytical methodologies are much more varied and plentiful: their two main tools are modeling and simulation or off-the-shelf catalogs. The use of models lends itself to modularity and combination into different processes. Nevertheless, this comes at a price, which is a higher input count. Such methodologies tend to provide competitive and innovative performance, yet some have reliability or control considerations [5, 8, 34, 37]. Since this has been observed in analytical modeling and simulation methodologies, their modularity could be a pathway to the addition of reliability analysis.

Analytical catalog-based methodologies, on the other hand, are great tools for detailed design

as they produce a [Bill of Materials](#). As such, their reliance on existing component databases hinders their innovative capabilities and reliability considerations. However, the databases provide an unrivaled certainty of design feasibility which the other methodologies cannot provide. Although control and safety considerations are mentioned [43, 46, 47], reliability has not been implemented in these types of methodologies. A summary table of these conclusions is displayed in Table 2.5.

Table 2.5: Design Methodologies State-of-the-art Findings

Methodology	Conventional	Innovation	Redundancy Affinity	Certainty
Empirical	~	X	X	X
Analytical Models and Simulations	~	✓	✓	X
Analytical Catalog-Based	✓	X	X	✓

The case study demonstrates there is a gap in the evaluation of design uncertainty as the design progresses and that redundancies affect the design in a major way. Reliability should be addressed as early as possible along the design phases, in a methodology with minimal inputs, yet sufficient design certainty. Empirical methodologies could be a great fit in the future, once redundancy effects can be estimated accurately through coefficients or once components will be readily reliable. Although the case study results demonstrate that the analytical modeling and simulation methodology provides subpar results for conventional designs, this is due to the case study restrictions which do not cover mission-related sizing, in which this method excels [8]. Moreover, its redundant results prove closer to the redundant catalog-based designs. Hence, analytical modeling and simulation methodologies are best for reliability implementation while preserving competitive performance capabilities, although their certainty of design feasibility should be improved.

Chapter 3

Controllability for Reliability

To correctly assess the effect of loss of control for multirotor UAVs, the controllability of such systems should be defined. This section outlines the controllability assessment methods of multirotor UAVs, potential improvements and its applications for reliability. Using the previous findings of Chapter 2, controllability will be implemented in an adequate design methodology and evaluated in a case study to establish its effectiveness at ensuring that resulting designs are resistant to rotor failure.

3.1 Multirotor Dynamics Model

To better define the effect of loss of control failures, the dynamics model of multirotor systems will be displayed in this section. The related state space model is displayed in Equation (3) below.

$$\dot{x} = Ax + Bu \quad (3)$$

Where x is the state vector, A is the state matrix, B is the inertia matrix and $u \in R^4$ is the virtual control input vector. For the purpose of this paper, the state will be defined as follows.

$$x = [h \ \phi \ \theta \ \psi \ v_h \ p \ q \ r]^T \quad (4)$$

Where h is the altitude (m), ϕ is the roll angle (rads), θ is the pitch angle (rads), ψ is the yaw

angle (rads), v_h is the velocity along the altitude (m/s), p is the roll rotational speed (rad/s), q is the pitch rotational speed (rad/s) and r is the yaw rotational speed (rad/s). This entails that both altitude and attitude will be considered within the scope of this research.

The particularity of multirotor control arises in its different configurations. Indeed, the u vector will always contain the following forces. For the purpose of this research work, under-actuated multirotor configurations are considered, where u is defined as:

$$u = [Z \ L \ M \ N]^T \quad (5)$$

Where Z is the vertical force (N), L is the roll moment (N/m), M is the pitch moment (N/m) and N is the yaw moment (N/m) acting on the UAV. These forces and moments are the result of both the propulsor forces and, in the case of hover conditions, the effect of gravity, as shown in Equation (6). For simplification purposes, the control state of multirotor will be defined based on hover conditions.

$$u = B_f f + D_{gravity} \quad (6)$$

Where $B_f \in R^{4 \times n}$ is the control effectiveness matrix, $f \in R^n$ is the propulsor force vector and $D_{gravity} \in R^4$ is the vector containing the gravity forces applied to the aircraft. The control effectiveness matrix is dependent on the multirotor configuration, geometry and rotors. It should be noted that, in the case of a quadrotor, this is a square matrix, but it is not always the case. Examples of control effectiveness matrices for various configurations are displayed in Appendix C, which consider only coplanar and symmetric configurations.

As of the f propulsor force vector shown in equation (6), its values normally vary between the maximal thrust the propulsor can provide and zero, since multirotor propellers are generally unidirectional. Nevertheless, exceptions exist [34], which could allow variable pitch rotors to be multi-directional and, hence, provide negative thrust when required. Nevertheless, such additions significantly increase mechanical complexity. For the case of this research, only unidirectional propellers will be considered.

3.1.1 Moore-Penrose Pseudo-Inverse

Controllability assessment methods shown in section 3.2 rely on the application of pseudo-inverse matrix computations, which will be outlined in this section. Pseudo-inverse allows inverting of the control effectiveness matrix B_f to define the rotor thrust commands from the virtual input vector u . As presented in Appendix C, the control effectiveness matrix B_f is a square matrix for a quadrotor, but this may not always be the case. Other multirotor configurations may produce rectangular matrices, which require pseudo-inverse. Such a matrix noted A^+ exists for any matrix but may either be a left or right inverse. Indeed, its definition depends on whether the columns or rows of the matrix A are more numerous. If the rows are more numerous than the columns, it is coined a tall matrix. This is a left inverse computed as shown in Equation (7). If the columns are more numerous than the rows, it is coined as a wide matrix. This is a right inverse computed as shown in Equation (8), which is the case in focus for this research work, as the addition of additional rotors makes the control effectiveness matrix B_f grow wider, as shown in Appendix C.

$$(A^T A)^{-1} A^T A = I, A^+ A = I \quad (7)$$

$$A A^T (A A^T)^{-1} = I, A A^+ = I \quad (8)$$

3.2 Controllability

The original concept of controllability dates to 1960, when Kalman's definition [55] became a landmark. Controllability defines the ability of a system to actuate all of its state dimensions. Multiple types of controllability exist, including null controllability, which refers to the ability of a system to return to its stable state, and reachability, the ability of a system to move to a certain other specified state, which may not be the stable state. These definitions, although dependent on controllability, rather refer to the stability of a system.

This approach is purely theoretical and cannot take faults or calibrating of a specific control loop into account, which should be addressed at a later design phase. Based on the state space equations

shown in Equation (3), the controllability of a continuous and linear time-invariant system can be assessed through the determination of the rank of the following controllability matrix [56].

$$C_M = [B \ AB \ A^2B \ \dots \ A^{n-1}B] \quad (9)$$

Then, if the resulting matrix C_M has full rank n , the system is deemed controllable for both the state and the specific time interval requirement.

Multirotor Controllability

For the sizing of multirotor UAVs, a few issues arise in the application of Kalman's controllability [55]:

- It is binary, a system is either controllable or not. A gradient-optimization algorithm nested within an analytical design methodology could not determine an optimization direction from a binary result and, thus, could not optimize for controllability.
- It does not take input disturbances into effect. As seen in Equation (6), the effect of gravity should be taken into account to determine the controllability of multirotor UAVs as well as the transfer of rotor forces into moments through the control effectiveness matrix B_f .
- It cannot be applied to complex non-linear systems. Multirotor UAVs require such nonlinearities considering they use unidirectional rotors. In such cases, the rank of the controllability matrix is not sufficient.

Thus, the following sections will outline the main applications of controllability to multirotor systems in terms of available control authority. Three different methods of assessing controllability are presented in the next sections, mainly the Attainable Control Set (ACS), Degree of Controllability (DoC) and Available Control Authority Index (ACAI).

3.2.1 ACS

The Attainable Control Set [4], and similar process the Attainable Moment Set (AMS) [57, 58] for the attitude only, are controllability methods that aim at developing a control polytope displaying

the possible maneuvers a system may perform. Considering the input vector of multirotor control from Equation (5), the dimensions of this polytope are thrust, roll, pitch and yaw. An example of such a polytope is demonstrated in Figure 3.1, although one of its dimensions was removed for illustration purposes.

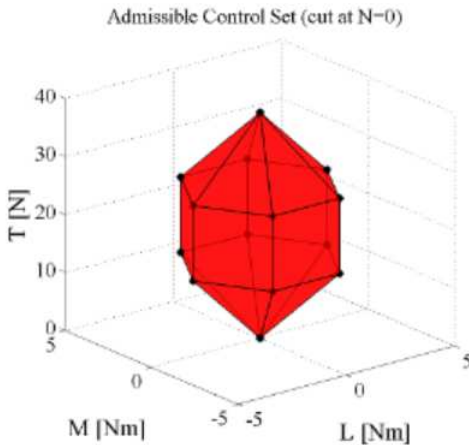


Figure 3.1: ACS Polytope [4]

This polytope is defined by the control effectiveness matrix B_f and u as shown in Appendix C, which alters for each multirotor configuration. Then, the failures of different propulsors are injected into the equations to observe the impact on the resulting polytope, as shown in Figure 3.2. This evaluation requires a projection on a two-dimensional plane, where the difference in radii between the fault-injected R_{fault} and the regular $R_{nominal}$ defines the controllability degradation ensued by the failure.

A variety [4, 57, 58, 59, 60] of multirotor works make use of the ACS or AMS. This method is a great tool to determine the effects of rotor failure due to loss of control and explore new rotor arrangements. This methodology applies the concept of reachability demonstrated in section 3.2. However, disturbances are harder to define. The projection on a two-dimensional plane are also quite computationally-heavy. Furthermore, the value of the ACS, although non-binary, cannot be easily translated to a physical counterpart. It would then be difficult to define a controllability requirement to optimize for.

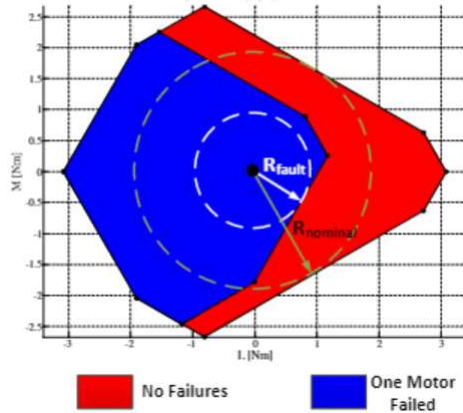


Figure 3.2: ACS Polytope after Fault Injection (2D Plane) [4]

3.2.2 DoC

The **Degree of Controllability** is an evolution of Kalman’s controllability [61, 6]. The **DoC** determines a recovery region around a stable state based on a specific recovery time. Hence, this method focuses on null controllability, determining the effort required for a system to return to a stable state within certain time limitations.

The **DoC** was not originally designed for multirotor in mind [6, 61], as opposed to the **ACS** and the **ACAI**. The original definition of it refers to modal systems such as satellite actuation [61]. Nevertheless, its applications to multirotor systems are plentiful [10, 62]. Its detailed methodology is defined in section 3.3.1. The applications of **DoC** tend to focus on strict attitude control since they observe the effects of different rotor degradation levels along a configuration, demonstrating that some rotors may be more critical than others for attitude control. The interesting addition within this methodology is the concept of recovery time, which could contribute to the definition of controllability requirements. Nevertheless, its computation time is significant due to the discretized simulation model required to compute the recovery region, comparable to the **ACS**.

3.2.3 ACAI

The **Available Control Authority Index** [63] is an evolution of the **ACS**. The **ACAI** defines a polytope similar to the **ACS** based on motor performance, the B_f matrix and external disturbances

to describe the effector potential. Then, the [ACAI](#) defines the largest four-dimensional sphere which may fit within that polytope from a disturbed center state. The versatility of this methodology comes from the ease to add disturbances and move the center of such a sphere within the [ACS](#), as shown in [Figure 3.3](#).

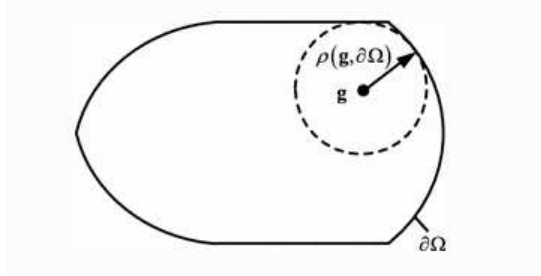


Figure 3.3: The Largest Enclosed Sphere within the [ACS](#) with Center g [5]

As such, this methodology is closer to the concept of reachability demonstrated in [section 3.2](#), as it evaluates the maximal physical capability of a system from a chosen initial point. Multiple different sources [[5](#), [63](#), [64](#)] refer to the [ACAI](#) to assess the controllability of various multirotor configurations. Mainly, the change in the order of rotors that spin counter-clockwise or clockwise to define the yaw moment can potentially increase controllability for attitude [[63](#)]. Moreover, the [ACAI](#) has been implemented in design methodologies before [[8](#)], leading to an increase in reliability. Nevertheless, this methodology still produces a controllability value with little physical meaning.

3.2.4 Summary

All controllability assessment methods have a similar methodology with a few crucial differences. The definition of the allowable control polytope or space is quite different in each method, although always required. These methodologies are compared to establish which is best for the assessment of the controllability of a multirotor [UAV](#) due to a loss of control within an analytical modeling and simulation sizing methodology. Findings from this exercise are summarized in [Table 3.1](#).

Table 3.1: Controllability Assessment Findings

Methodology	Allow Visualization	Includes Disturbances	Time Consideration	Computation Cost
ACS	✓	X	X	X
DoC	X	✓	✓	X
ACAI	X	✓	X	✓

Although the ACS is a great visualization tool, applying gravitational disturbances to the control polytope is quite complex compared to its counterparts. The projections required are computationally heavy, which is also an issue shared by the DoC. The most computationally efficient methodology is the ACAI, however, its end value has little physical properties. On the other hand, the DoC may provide a recovery time requirement, which could allow for even comparison between different designs and defines physical requirements related to controllability. Hence, the Degree of Controllability is chosen for the contribution of this research work due to its ease of implementing disturbances and its time-dependent potential while attempts will be made at mitigating its high computation requirements.

3.3 Contribution

The contribution is divided into two parts: the development of a script that may assess the DoC of multirotor UAVs and the implementation of it within the analytical design methodology's MDO framework.

3.3.1 Multirotor DoC Methodology Development

The DoC's original methodology and a few required changes will be outlined in the current section to define the application of the controllability assessment method to multirotor systems.

DoC Methodology

This methodology is equally related to state space control theory, shown in Equation (3). However, the DoC requires additional constraints on the virtual control input vector u . Indeed, u should

be normalized, as shown in Equation (10) to maintain the symmetry of the state polytope around the null state.

$$|u(t)| \leq 1 \quad (10)$$

In the original definition written by Viswanath et al. [61], the recovery region for a pre-selected time T is outlined as per Equation (11).

$$R = x(0) | \exists u(t), t \in [0, T] \text{ for } i = 1, 2, \dots, m \ni, x(T) = 0 \quad (11)$$

And, the DoC value is defined as per Equation (12).

$$\rho = \inf \| x(0) \| \forall x(0) \notin R \quad (12)$$

In summary, the recovery region spans the potential of the normalized effector $u(t)$ within the time T . It states that, at any point within this space, there must exist a normalized effector vector that may bring back the system to its stable state within time T . Then, the DoC, shown as ρ in Equation (12), is a measure of the size of the recovery region.

To be properly computed, this recovery region must be discretized, as advised by Klein et al. [6]. The first step is to define the solution to the state space Equation (3). This solution is outlined in Equation (13).

$$x(t) = e^{At}x(0) + e^{At} \int_0^t e^{-A\tau} Bu(\tau) d\tau \quad (13)$$

The time T is then divided into N equal intervals ΔT . Using the definitions shown in Equation (14), Equation (13) is then altered to Equation (15) through discretization.

$$x_k = x(k\Delta T), u_k = u(k\Delta T) \quad (14)$$

$$x((k+1)\Delta T) = e^{A\Delta T} x_k + e^{A\Delta T} \int_0^{\Delta T} e^{-A\tau} Bu_k d\tau \quad (15)$$

To make these equations simpler, the matrices G and H are defined in Equations (16) and (17). Then, the equivalent of Equation (15) is shown using the new matrices in Equation (18).

$$G(\Delta T) = e^{A\Delta T} \quad (16)$$

$$H(\Delta T) = B \int_0^{\Delta T} e^{A(\Delta T - \tau)} d(\Delta T - \tau) \quad (17)$$

$$x_{k+1} = Gx_k + Hu_k \quad (18)$$

After an iterative substitution, a generalized expression can be derived from Equation (18) to display the final state of the system, shown in Equation (19). Since observing null controllability is this research work's aim, x_N will be set to zero to obtain Equation (20), where u is defined in Equation (21) and F is defined as in Equation (22).

$$x_N = G^N x_0 + \sum_{i=0}^{N-1} G^{N-1-i} H u_i \quad (19)$$

$$x_0 = -G^{-N} F u \quad (20)$$

$$u = [u_0 \ u_1 \ \dots \ u_{N-1}]^T \in R^{N \times m} \quad (21)$$

$$F = [G^{N-1} H | G^{N-2} H | \dots | H] \quad (22)$$

The boundary of the discretized recovery region is formed by hyperplanes which form a control state polytope. This is an estimation of the actual recovery region [6]. In the case of a multirotor, this polytope would cover the dimensions of state vector x .

To explain this concept further, an assumed three-dimensional recovery region is shown in Figure 3.4. The goal of the DoC is to determine the shortest distance from the stable state to the edges of

the recovery region for each of its dimensions. After going through a linear transformation, shown in Equation (20), parallel lines from the initial control environment maintain their parallel nature. Along a singular dimension, two segments are parallel extremums. Moreover, due to the nature of the input vector u , they should be symmetric about the center. Hence, the definition of the DoC becomes the minimum of all the perpendicular distances between the sets of parallel hyperplanes in the discretized recovery region.

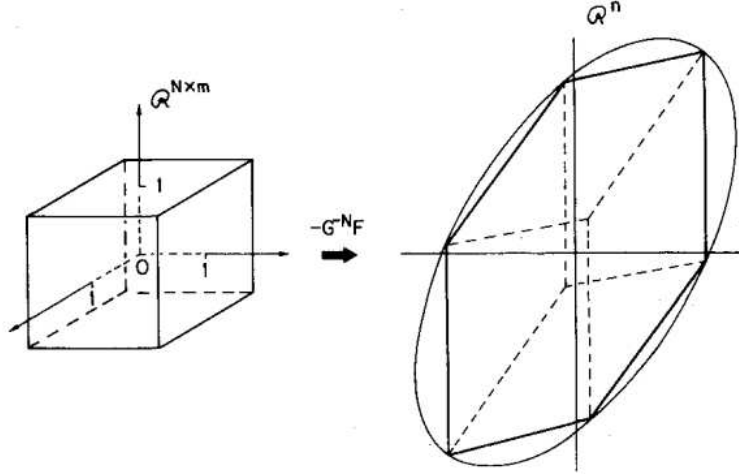


Figure 3.4: Control State Polytope and Recovery Region Illustrated in Three Dimensions [6]

The linear transformation explained above is summarized in Equation (23). The combinatory matrix computation begins with the definition of u_1 and u_2 in Equation (24). The $n - 1$ dimensional boundary of the polytope can be defined by fixing $(N \times m) - (n - 1)$ of the values of u [6]. The remainder, u_1 , can then vary between its extreme values, -1 and 1, and should contain $(n - 1)$ elements.

$$x_0 = Ku, \text{ where } K = -G^{-N}F \quad (23)$$

$$u_1 \in R^{n-1}, u_2 \in R^{(N \times m) - (n-1)} \quad (24)$$

Then, to determine the hyperplanes, Equation (25) partitions the K matrix according to Equation (24). Where $N \times m$ refers to the original control space dimensions and n refers to the dimensions

of the recovery region, as shown in Figure 3.4. Then, there exists a normalized non-zero vector of dimension n which is determined through Equation (26). Finally, the perpendicular distances between hyperplanes are calculated through Equation (27).

$$x_0 = [K_1 \ K_2] \begin{bmatrix} u_1 \\ u_2 \end{bmatrix}, \quad x_0 = K_1 u_1 + K_2 u_2 \quad (25)$$

$$\xi^T K_1 = 0 \quad (26)$$

$$\rho = \frac{|\xi^T K_2 u_2|}{\sqrt{\xi^T \xi}} \quad (27)$$

Multiple values of ρ are computed for all the different possible combinations of K and u shown in Equations 25 and 24 and the minimum is set to be the **Degree of Controllability** [6]. If that value is higher than zero, the system is deemed controllable.

Application to Multirotor

The main issue to tackle for use of the **DoC** for multirotor refers to Equations 6 and 10. This methodology is based on the normalization of the virtual control input vector $u(t)$, which, as seen previously, can only be unidirectional due to multirotor propellers, must include transitional matrices such as B_f and must include gravitational disturbances. This contradicts with Equation (10), hence, alternatives for asymmetrical effector vectors must be explored.

One such alternative, written in Mandarin [65], dictates the implementation of the **DoC** to multirotor in detail. To validate it, it was verified with other sources [10, 62] computing the **DoC** for multirotor **UAVs** with similar methodologies.

The main difference with the initial methodology of the **DoC** is the formulation of a new input vector based on the asymmetric values of both a , b and a new center state related to them. The new input vector and this center state, defined as x_p , are shown in Equation (28) and (29).

$$u(t) \in [a, b]^m \in R^m \quad (28)$$

$$x_p = KU_c, U_c = \begin{bmatrix} \frac{a+b}{2} \\ \frac{a+b}{2} \\ \dots \\ \frac{a+b}{2} \end{bmatrix} \quad (29)$$

For the case of multirotor UAVs, the vectors a and b are defined as in Equation (30).

$$a = f_{min} + B_f^{-1}D_{gravity}, b = f_{max} + B_f^{-1}D_{gravity} \quad (30)$$

Where f_{min} and f_{max} are respectively the minimal and maximal force vectors provided by the rotors and B_f^{-1} is the inverse (or pseudo-inverse if rectangular) of the control effectiveness matrix. This ensures that the input vector range covers the disturbances associated with hover conditions and the strict positivity of the effectors. Moreover, failure injection of the rotors is now a possibility by changing the values within the f_{max} vector.

Changes must also be applied to the computation of ρ , previously calculated as in Equation (27). These are demonstrated in Equations (31), (32) and (33) [65], where $\rho_{multirotor}$ is the DoC value.

$$\rho = (\text{sign}(\xi^T K_2))^T \xi^T K_2 \frac{b-a}{2} \quad (31)$$

$$l = |\xi^T x_p| \quad (32)$$

$$\rho_{multirotor} = \rho - l \quad (33)$$

Hence, the DoC can now be computed for multirotor UAVs with respect to disturbances that illustrate their hover conditions. The use of a state as shown in Equation (4) permits both altitude and attitude control. The following section will outline the main results from the DoC computations and their validation.

3.3.2 DoC Computation and Results

Within this section, the main challenges associated with the computation of the DoC within a script will be described along with initial validation and results with fault injection for various multirotor configurations.

DoC Script Development

Considering the DoC is discretized through integration as shown in Equation (13), the script is designed around the use of symbolic variables and matrix computations. For such reasons, the initial draft of the script was developed on MATLAB. Eventually, a python script was required for the implementation into the analytical design methodology.

DoC Script Validation

The script was validated in association with the original reference, written in Mandarin [65]. However, their DoC evaluation did not include altitude, which means no hover disturbance $D_{gravity}$ is included, as shown in Equation (30). Nevertheless, after modification of the script to only include roll, pitch and yaw, the default configuration for a standard hexarotor provided the same result as the source [65]. The DoC computation script was also validated with comparison with the ACAI [8] since this version includes altitude controllability.

DoC Script Results

Using the previously described script, the effects of rotor failure for various multirotor configurations were evaluated. The designs were obtained using the analytical design methodology [7] shown in section 2.3.1. Appendix D showcases the design requirements and performance while the DoC is shown in Figure 3.5. The octorotor, coaxial quadrotor and coaxial hexarotor were demonstrated to be resistant to rotor failure. In the case of dual rotor failure, where only the most critical failure combination is demonstrated, only the coaxial hexarotor is resistant.

Similarly to the accuracy analysis presented by Klein et al. [6], the DoC without any failures is computed in Figure 3.6 for a variety of recovery times and time steps requirements for the hexarotor

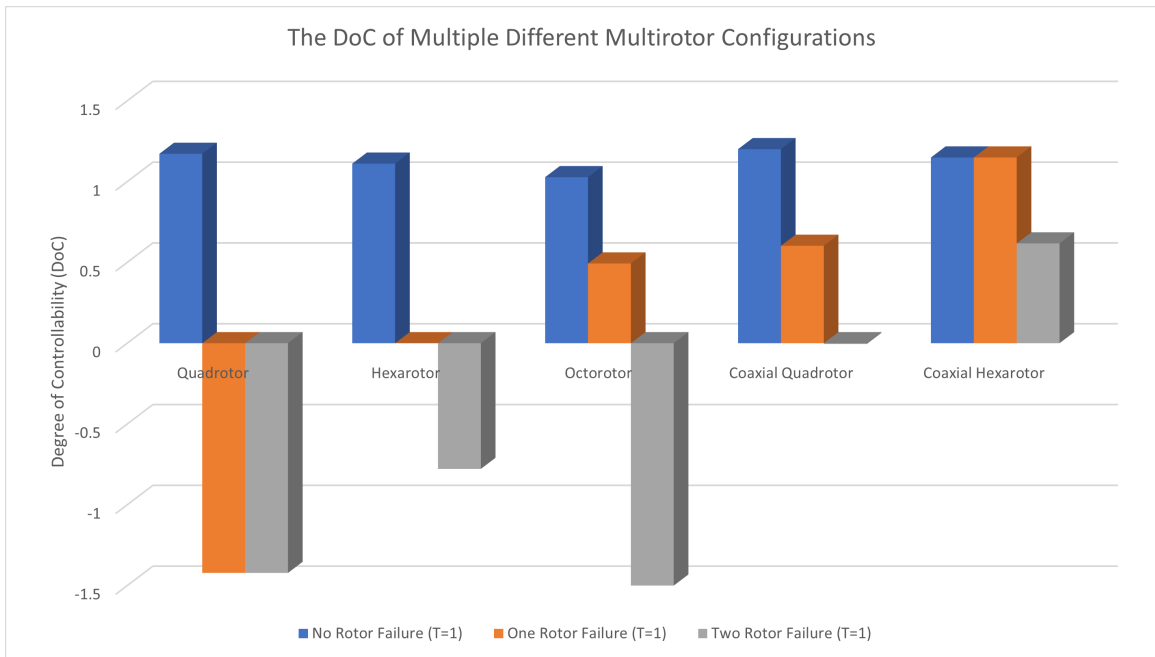


Figure 3.5: The DoC of Multiple Different Multirotor Configurations

design shown in Figure 3.5. It is concluded that the resulting percent error at two time segments is around 10% when compared to six time segments around a unity recovery time. It should also be noticed that, for a controllable configuration, the trends evokes an asymptote along the total maneuvering time axis. This trend will be further explored in the case studies to evaluate if the recovery time requirement may be used to quantify once a multirotor UAV's becomes uncontrollable. As for the time segments, they induce a steep loss in computing efficiency, displayed in Figure 3.7. Due to the high computing time, only two time segments will be considered during the case studies.

3.3.3 DoC Implementation in Analytical Sizing Methodology

This section will outline the implementation of the DoC in the previously chosen analytical methodology [7] displayed in section 2.3.1.

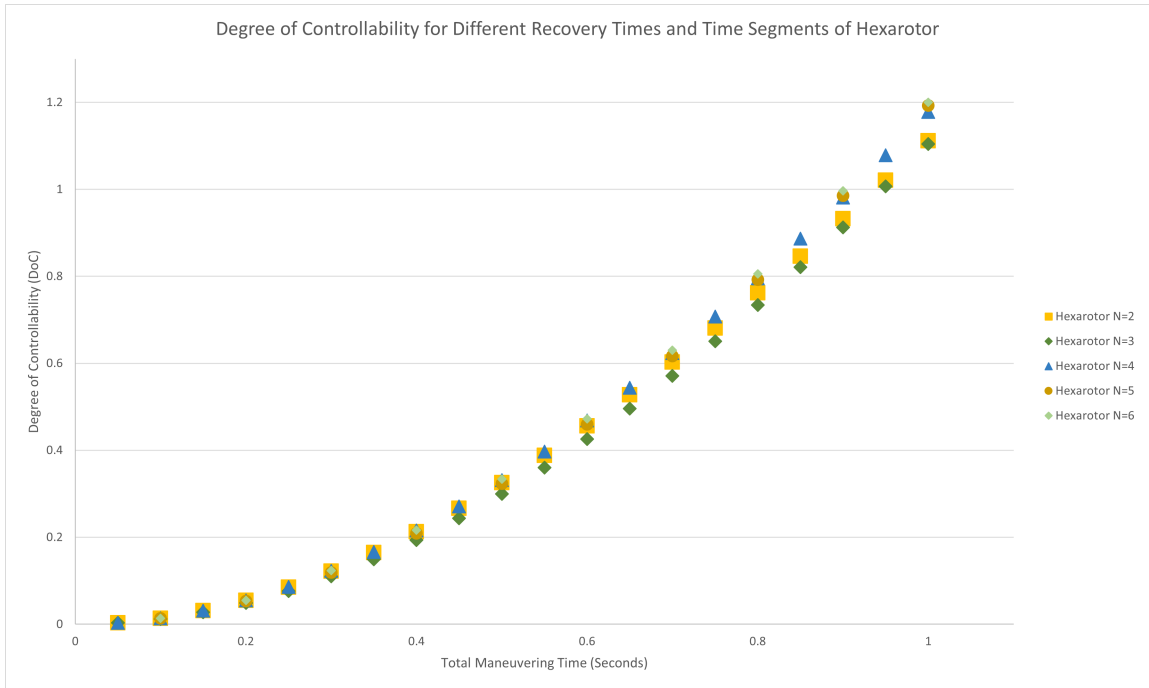


Figure 3.6: DoC for Different Recovery Times and Time Segments of Hexarotor

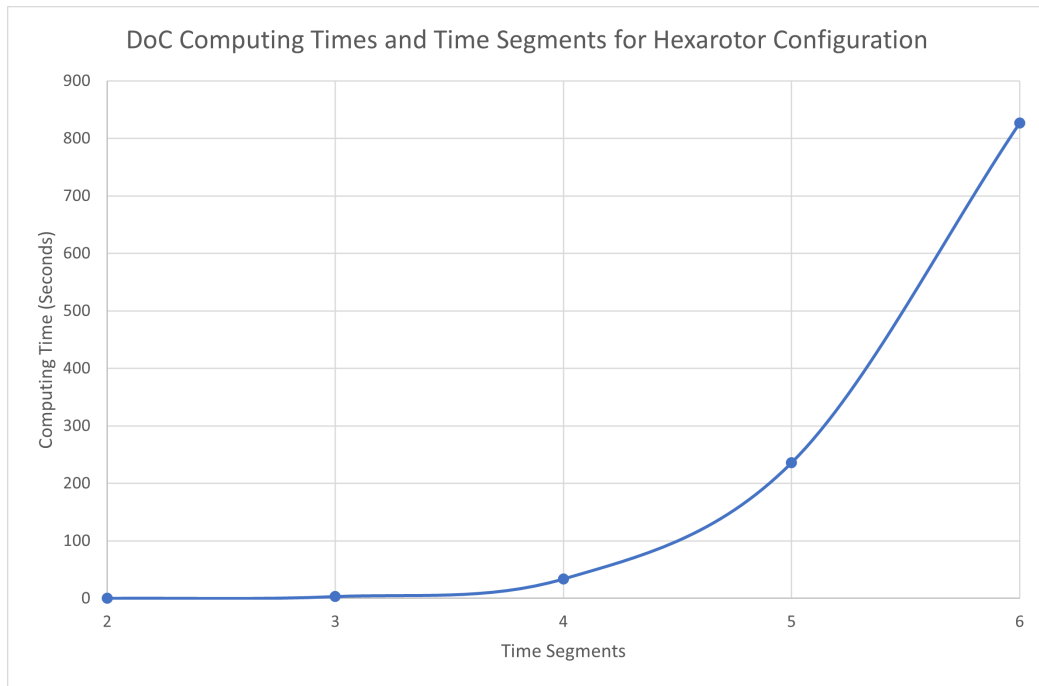


Figure 3.7: DoC Computing Times for Hexarotor Configuration

Analytical Sizing Methodology Framework

The [Multidisciplinary Optimization](#) analytical design methodology [7] utilizes OpenMDAO [54] and derived software, OpenOAD [66]. The methodology is an object-oriented python package including modules for each of the multirotor UAV's components. It can be run on web-based interactive computing software such as JupyterLab or Jupyter notebooks.

DoC Implementation

The DoC is added to the framework as a new component module tackling controllability. This module and its outputs can thus be included in the design variables and constraints of the methodology. Mainly, an additional constraint is added for the value of the DoC to ensure it is greater than zero in the case of one rotor failure. Considering the software makes use of gradient-based optimization, it can define a gradient from the DoC values and optimize it accordingly. Moreover, a secondary objective function is defined for the analytical methodology's MDO framework. Both the mass minimization and DoC maximization goals were combined in a Pareto optimization format [24].

The dependencies between the different modules part of the methodology and the newly added control module are shown in Figure 3.8. Additionally, the main inputs of the module are shown in a similar format in Figure 3.9. These include, in order, a binary value defining if the configuration is coaxial, the number of propellers, the maximum thrust, the arm length, the MTOW, the motor mass, the propeller mass, the required recovery time and the requirement for time segments. On each iteration, the analytical methodology makes changes to the inputs and the DoC is computed. The computation time varies based on the configuration chosen and the time segments.

Thus, the implementation of the DoC should allow the evaluation and optimization of multirotor UAVs for both performance and reliability for loss of control failures. This will be further explored in the case study which follows.

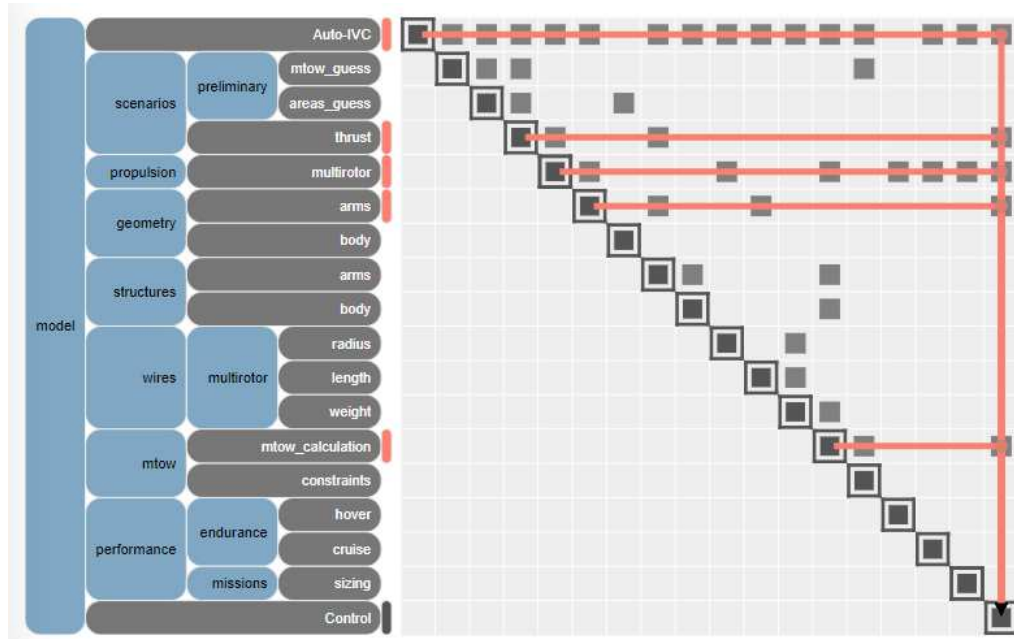


Figure 3.8: The Inter-Dependencies Between the Control Module and its Counterparts [7]



Figure 3.9: The Inputs Required for the Control Module [7]

3.4 Case Studies

The following section validates the main contribution of this research work, which includes the implementation of a controllability assessment into an analytical sizing methodology. This resulting methodology, which optimizes for both performance and reliability, will be compared in a case study to assess the effects of heightened controllability on performance, determine the differences between the ACAI and the DoC assessments, and evaluate the potential of innovative design features.

3.4.1 Methodology

Three different cases are to be investigated to properly convey the opportunities offered by the contribution. The full case design requirements are shown in Table 3.2.

Table 3.2: Controllability Case Study Requirements

Design Requirements	Effect of Controllability	ACAI Comparison	Design Features Exploration
Payload (kg)	10	20	10
Number of Rotors	8	8	6
Coaxial	Yes	Yes	No
Maximum T/W	2	1.6	2
Climb Height (m)	30	122	122
Climb Speed (m/s)	5	3	3
Hover Time (min)	10	0.5	10
Cruise Range (km)	N/A	25	N/A
Emergency Diversion (km)	N/A	12.5	N/A
Recovery Time (sec)	1	0.5, 1, 2	1
Time Steps	2	2	2

Effect of Controllability

The first case will inquire about the differences between two products with similar design requirements. However, one will be optimized for minimal mass, another for maximum Degree of Controllability and a third one, using Pareto optimization [24], will optimize both. The results are expected to showcase the performance cost of improved controllability.

ACAI Comparison

The second case will be a comparison with the results obtained by Liscouet et al. [8] during their reliability analysis based on the ACAI. The results should demonstrate the practical use of the recovery time requirement.

Design Features Exploration

Finally, a third case will display the use of innovative design features and display their controllability results. Mainly, the effect of variable pitch propellers will be explored to test the flexibility of the design tool to new innovative sizing approaches.

3.4.2 Results

Effect of Controllability

The results of the designs are shown in Figure 3.10. All designs are controllable after a rotor failure, however, the second and third cases have a significantly increased DoC. The difference between their controllability values and computing time is showcased in Table 3.3. Figure 3.10 highlights that maximized controllability has a steep cost on performance, which may increase the MTOW by up to 68%. Table 3.3 demonstrates that the objectives which consider the DoC have significantly higher computing times. This is due to the computing time of a single function evaluation of the DoC, which may take around two and a half minutes. These results demonstrate the range of optimization which is possible within the contribution using Pareto optimization [24] at the cost of computing time.

Table 3.3: DoC and Computing Time of Effect of Controllability Case

Objective Function	Minimize Mass	Maximize DoC	Optimize Both
Degree of Controllability	0.603	1.016	0.894
Computing Time	1.6 seconds	3.7 hours	5.1 hours

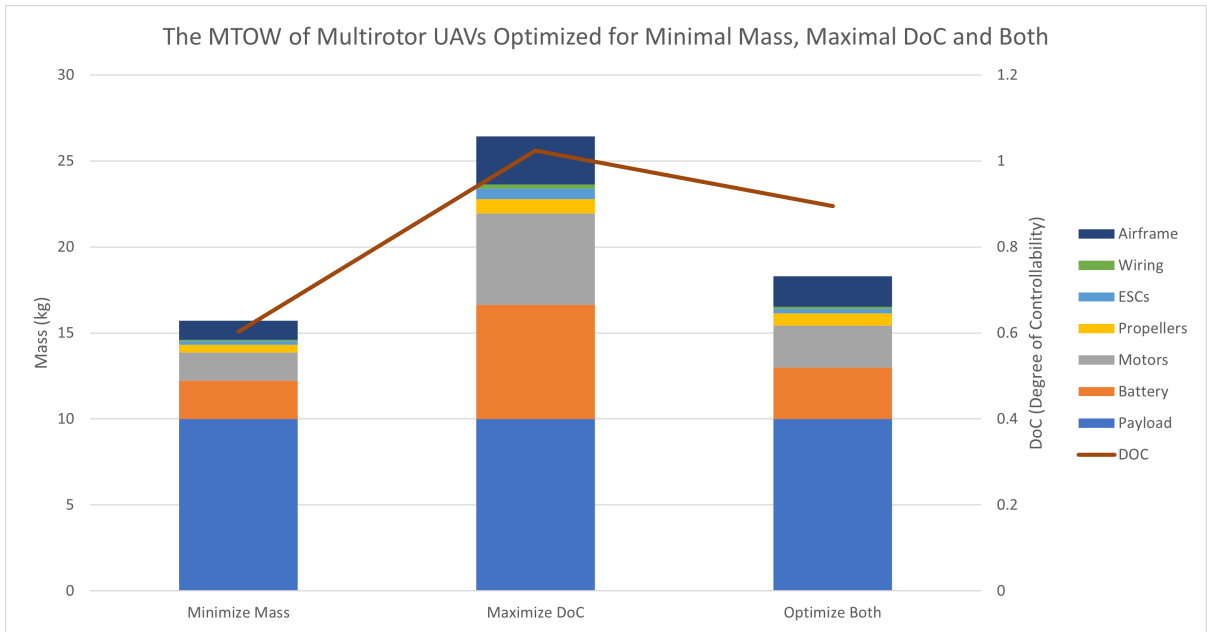


Figure 3.10: The **MTOW** of Multirotor **UAVs** Optimized for Minimal Mass, Maximum **DoC** and Both Objective Functions

ACAI Comparison

Through the use of failure case sizing and the **ACAI**, Liscouet et al. [8] defines reliable multirotor designs, one of which will be the reference for this case. In Figure 3.11, the **MTOW** of each coaxial quadrotor is shown. It was found that changing the recovery time had no effect on the resulting design, as the **DoC** scales with the recovery time. Although it would seem intuitive that a multirotor **UAV** with a smaller reaction time should be more performant, there does not exist a recovery time for which a controllable design will obtain a negative **DoC**, as shown in the asymptote observed in Figure 3.6. Hence, the time dimension of the **DoC** may not lead to a comprehensible and practical high-level requirement without further alteration of the methodology, which will be addressed in the findings. Furthermore, the inclusion of the constraint on the **DoC** led to the same results as the reference, which is already fault-tolerant. Table 3.4 showcases the **DoC** value for each of the designs shown in Figure 3.11.

Table 3.4: DoC and Computing Time of ACAI Comparison Case

Design	Reference	DoC > 0	Maximize DoC		
Recovery Time (sec)	1	1	0.5	1	2
Degree of Controllability	0.2186	0.2186	0.156	0.332	1.012

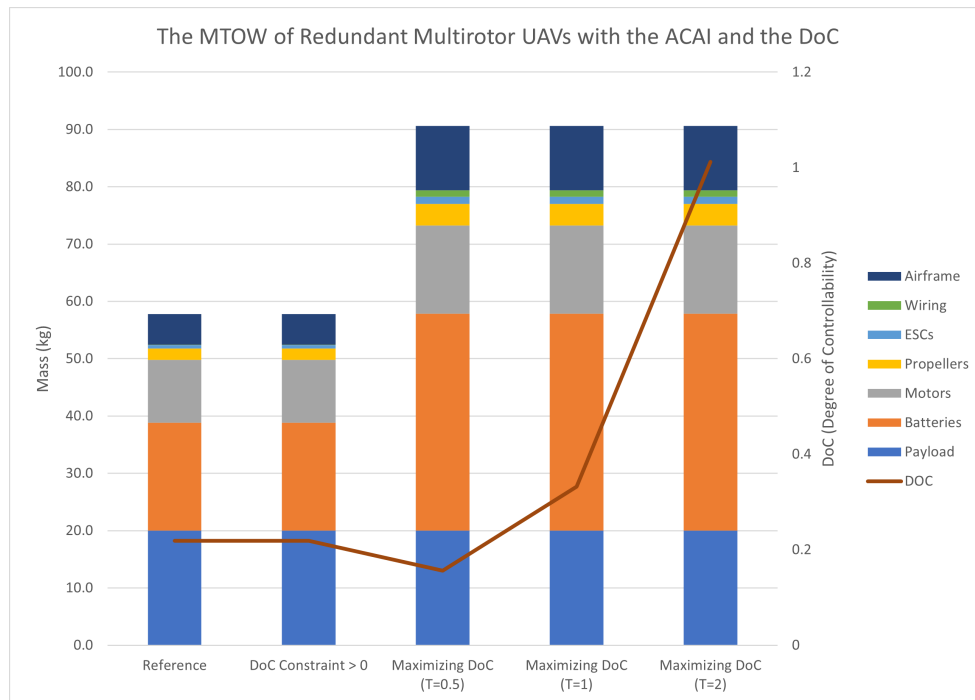


Figure 3.11: The **MTOW** of Redundant Multirotor **UAVs** with the **ACAI** and the **DoC**

Design Features Exploration

As seen in Table 3.5, a typical hexarotor, which is non-resistant to rotor failure for both altitude and attitude control, could become resistant due to the implementation of variable pitch propellers. Indeed, the MTOW of a typical hexarotor design is shown in Figure 3.12. The analytical methodology used for this case study cannot evaluate the effect of variable pitch propellers, nevertheless, the DoC of a hypothetical design with similar features as the traditional design and variable pitch propellers can be computed. As shown in Table 3.5, the DoC of a hexarotor can be made positive by expanding the range of the input vector a shown in Equation (30) to include negative inputs.

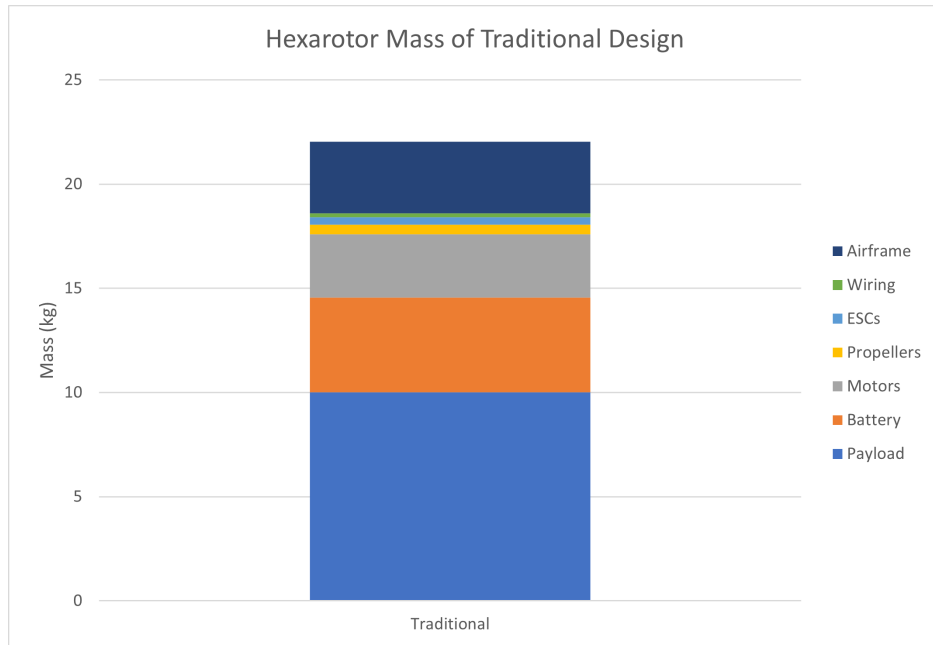


Figure 3.12: Hexarotor Mass of Traditional Design

Table 3.5: DoC of Design Features Exploration Case

Design	Traditional	Variable Pitch Propellers
Degree of Controllability	-1.78×10^{-15}	0.605

3.5 Findings

The exploration of controllability led to its definition as a tool to assess if a design can be resistant to rotor failure and prevent loss of control. The ACS, ACAI and DoC each demonstrated various methodologies to define the controllability of multirotor UAVs. The DoC is the best fit for implementation within an MDO analytical modeling and simulation design methodology that uses gradient-based optimization.

The DoC is successfully modified to include gravitational disturbances and accommodate for altitude controllability evaluation. This new control module, as part of the analytical methodology, can compute the DoC on each separate iteration. Its precision is limited by the time segments chosen to evaluate the controllability. However, this process significantly increases the design method's computing time, even more when considering extra time segments.

The case studies demonstrate the potential uses of the control module within an optimization framework. The DoC module can ensure a design is tolerant to rotor loss and optimize a multirotor UAV for maximal controllability. The best scenario remains nonetheless to optimize for both mass minimization while maintaining a constraint on the DoC, since maximizing the controllability can hinder competitive performance. However, the effect of the recovery time requirement is not as expected. As the DoC scales with recovery time, it may not be used as a high-level design requirement since the most controllable design should be the same, no matter the pre-assigned recovery time. There is yet potential in the use of the recovery time in future evolutions of this work. As an example, recovery regions associated with specific maneuvers in the future could be independent of time, allowing the existence of minimal recovery time requirements. If that requirement is not met, the recovery region scaled by the DoC and recovery time could not surpass the boundary of the independent recovery region displaying required maneuvers. The case study equally demonstrates the ability to compute the controllability of innovative design features, such as variable pitch propellers. Varieties of different configurations and propulsion options could be evaluated in the future with this tool.

Chapter 4

Conclusion

To close, fully-electric multirotor UAVs are at the mercy of loss of control failures which harm their reliability. The implementation of redundancies in the sizing of multirotor UAVs is detrimental to their competitive performance. Hence, a solution to produce both performant and reliable designs is investigated.

The design methodologies of multirotor UAVs can be classified two-fold, empirical and analytical. Empirical methodologies prove to be estimation tools for early conceptual design while analytical methodologies can either focus on modeling and simulation or off-the-shelf catalogs. Analytical modeling and simulation processes show great promise to design innovative and redundant multirotor. On the other hand, analytical catalog-based methodologies are best used in the detailed design phase due to their high-fidelity results.

Loss of control failures for fully-electric multirotor UAVs can be mitigated by implementing a controllability assessment within their design process. However, traditional controllability assessments cannot be readily applied to multirotor systems and analytical modeling and simulation methodologies. Among the alternatives, the ACS, ACAI, and DoC, the Degree of Controllability is the best fit for the implementation within the multirotor design process since it could provide a recovery time requirement and the easy inclusion of disturbances.

The DoC is modified to include the gravitational and configuration-induced disturbances to its stable hovering state and then implemented within an MDO analytical design methodology. Hence, the resulting methodology produces competitive designs resistant to rotor failure. However, the use

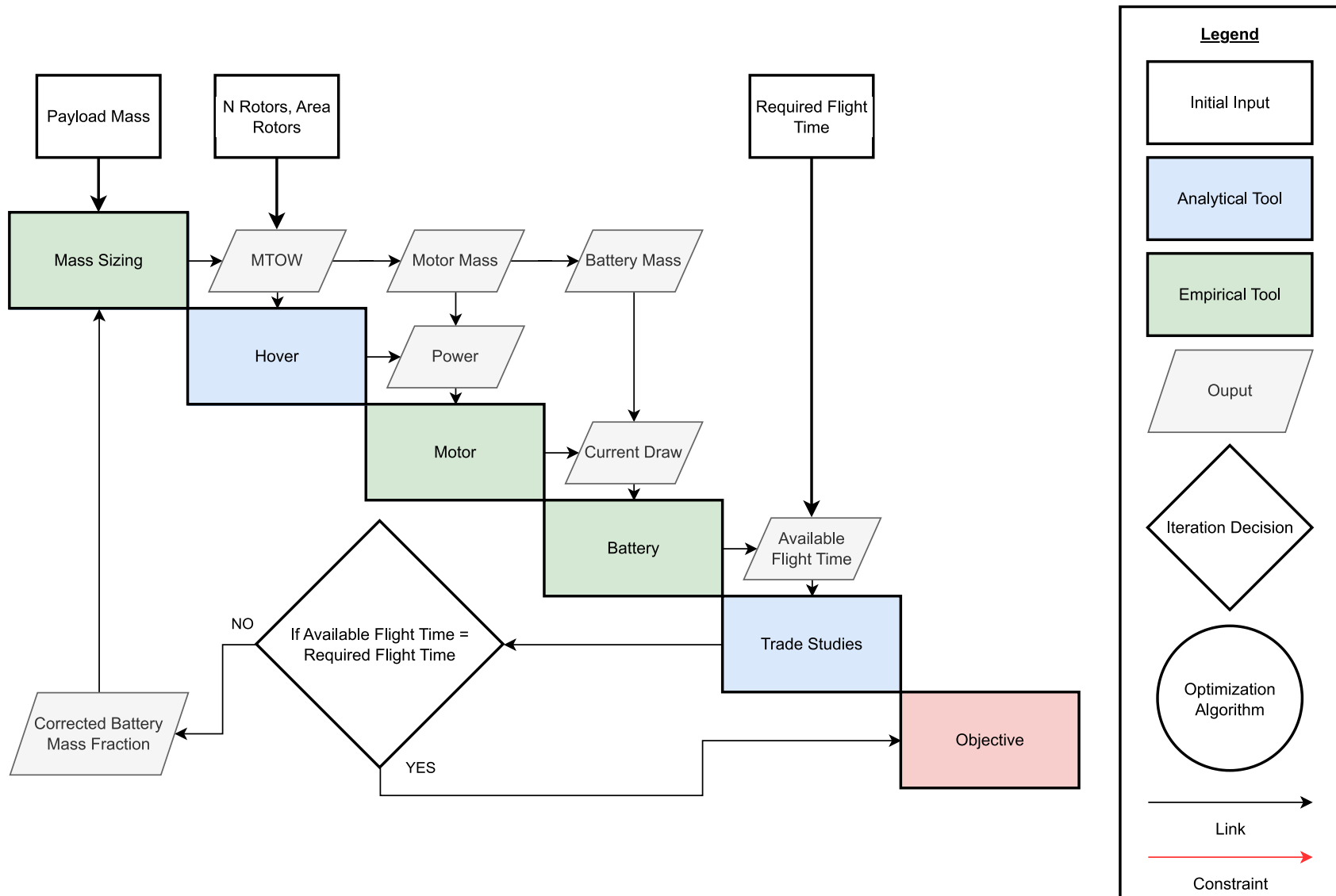
of an aircraft-level recovery time requirement may not yet be implemented within the methodology due to its inherent scaling of the DoC. Future works should alter the controllability assessment to include reference recovery regions independent of time, from which recovery time conclusions could be drawn. The main limitations of the implementation reside within its tremendous computing time, which may be optimized in future works.

Therefore, multirotor UAVs may be optimized for both competitive performance and heightened reliability. Such practices may lead multirotor UAVs to fly overhead in the near future.

Appendix A

Design Methodologies N_2 Diagrams

The figures within this appendix represent the multirotor UAV design methodologies which are part of the case study comparative analysis shown in section 2.3. Each includes an N_2 diagram [53], which are flowcharts to describe the general process of a design methodology. The three examples include the empirical methodology [3] shown in Figure A.1, the analytical modeling and simulation methodology [7] in Figure A.2 and the analytical catalog-based methodology [46, 47] in Figure A.3.

Figure A.1: N_2 Diagram of the Empirical Methodology

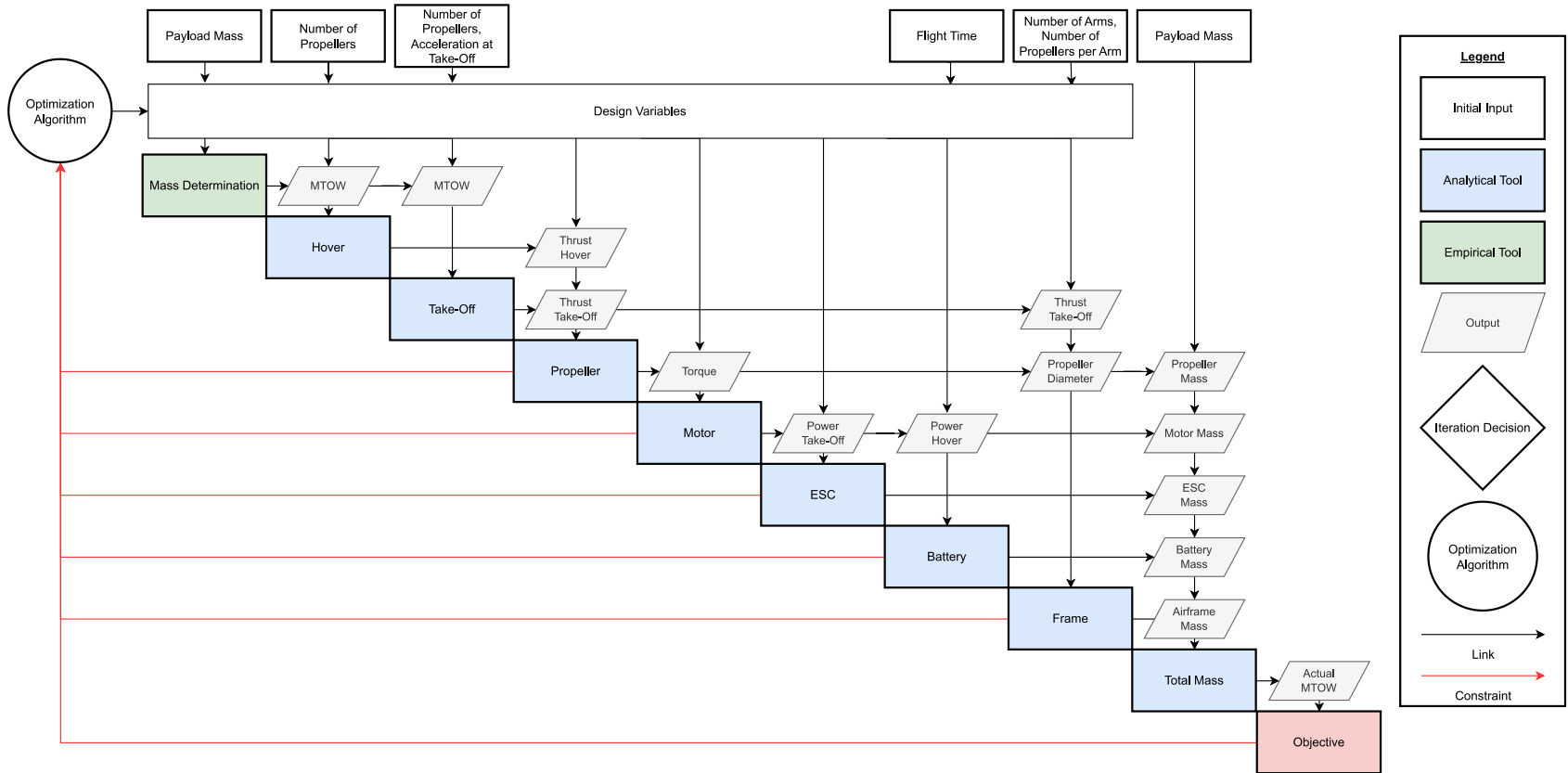


Figure A.2: N_2 Diagram of the Analytical Modeling and Simulation Methodology

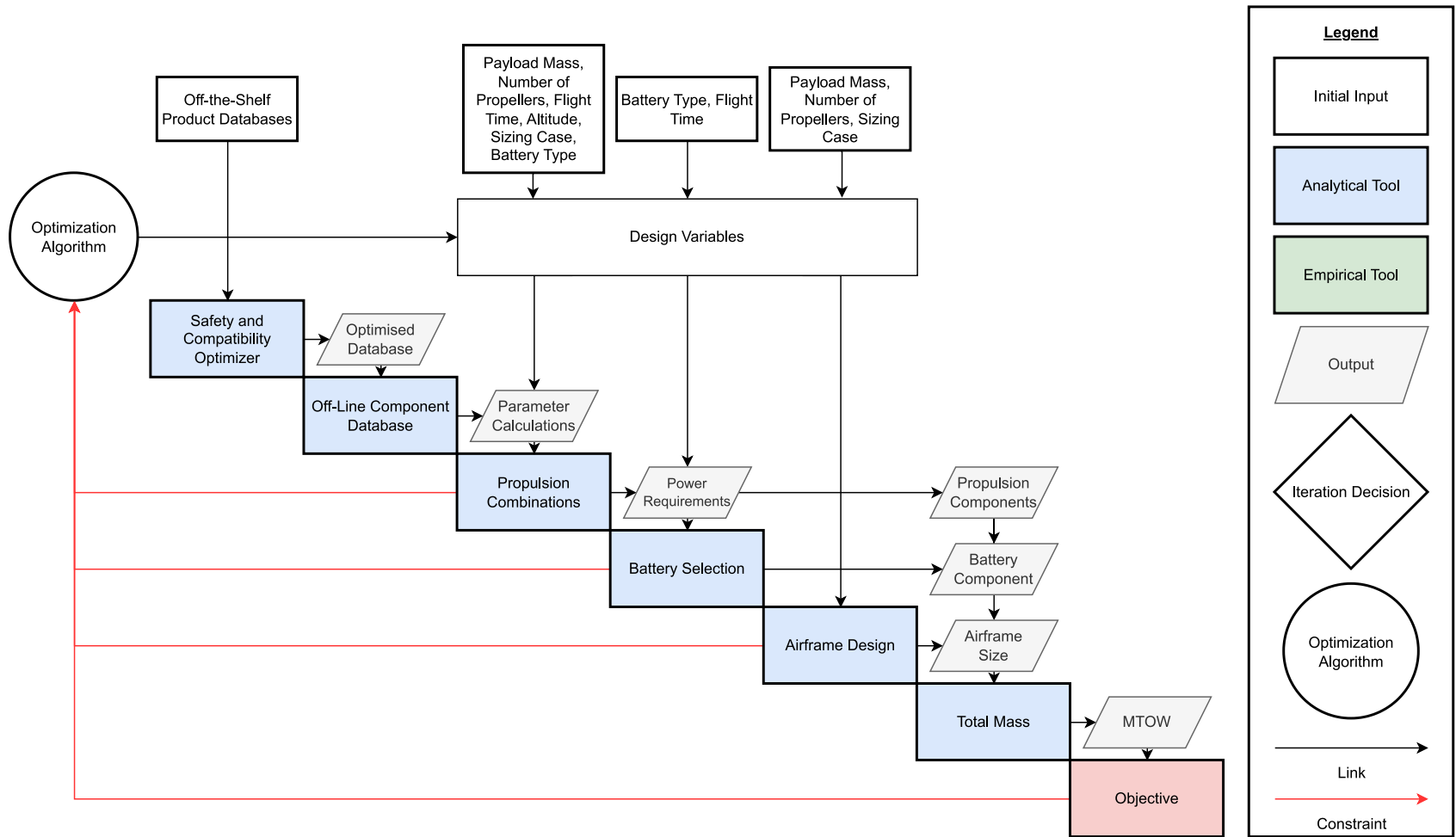


Figure A.3: N_2 Diagram of the Analytical Catalog-Based Methodology

Appendix B

Design Methodologies Input Analysis

This section outlines the major summarized inputs of each of the multirotor design methodologies part of the case study in section 2.3. Table B.1 displays the legend of the input Table B.2, which refers to the optimization framework shown in section 2.1.1. Certain design parameters may enact multiple functions from the ones displayed in Table B.1.

Table B.1: Legend of Design Methodologies Input Analysis

Letter	Function
I	Input
P	Parameter
V	Design Variable
C	Design Constraint
O	Output

Table B.2: Design Methodologies Input Analysis

Parameter	Empirical	Model and Simulation	Catalog-Based
Mission-Related			
Mission Segments		I	
Mission Type			I
Flight Time	I	I	I/V
Cruise Speed		I/V	V/O
Air Density	P	P	P
Altitude	P	I/C	I/C
Multicopter Drag Coefficient		C	C
Range		C/O	O
Emergency Diversion Range		C/O	
Propulsion			
Battery Energy Density	P	P/C	C
Battery Technology Type			I
Battery Nominal Voltage	P	V	V
Battery Depth of Discharge	P	C	C
Battery Cell Number		V/O	V/O
Battery Volume		V/O	
ESC Efficiency		P	P
Payload Power		I	
Motor Current Draw		C	C
Motor Max Torque		V/O	C
Rotors			
Number of Rotors	I	I	I
Rotor Radius	I	V/O	V/O
Coaxiality	I	I	I
Rotor FM	P		
Rotor BEMT Parameters		P/V	P/V
Mass			
T/W	P	I/C	V
Payload Mass	I	I	I
Battery Mass	V/O	V/O	V/O
Propulsor Mass		V/O	V/O
Avionics Mass		V/O	V
Structures Mass		V/O	V
MTOW	V/O	V/O	V/O
Geometry			
Arm Geometry		V/O	V/O
Multicopter Projected Area		P	O
Arm Inner/Outer Diameter		V/O	
Additional Modules			
Inter component Efficiencies			V
Component Database			V/O
BoM			O

Appendix C

Control Effectiveness Matrices

The control effectiveness matrices B_f for various multirotor configurations are shown in the following sections. These are the configurations included within the DoC assessment defined in Chapter 3. The numbering of the rotors for each configuration is shown in Figure C.1. For each subsequent control effectiveness matrix, d refers to the length of the multirotor UAV's arms (m) and j refers to a constant defining the effect of a rotor's spin on the yaw of the aircraft.

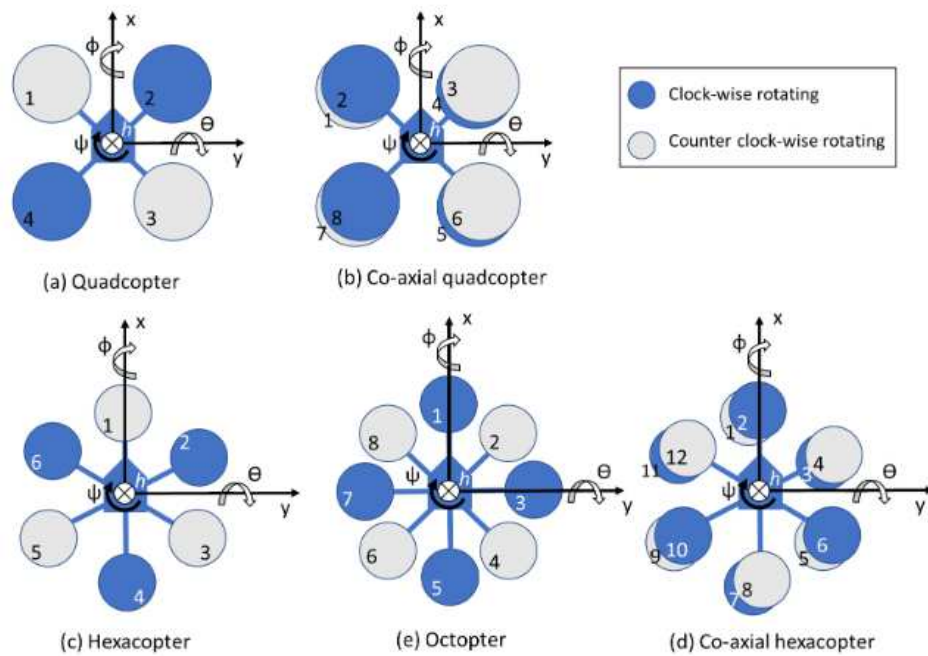


Figure C.1: Multirotor Configurations [8]

C.1 Quadrotor

Simple

The simple quadrotor control effectiveness matrix is shown in Equation 34.

$$B_f = \begin{bmatrix} 1 & 1 & 1 & 1 \\ d & -d & -d & d \\ d & d & -d & -d \\ j & -j & j & -j \end{bmatrix} \quad (34)$$

Coaxial

The coaxial quadrotor control effectiveness matrix is shown in the following Equation 35.

$$B_f = \begin{bmatrix} 1 & 1 & 1 & 1 & 1 & 1 & 1 & 1 \\ \frac{d\sqrt{2}}{2} & \frac{d\sqrt{2}}{2} & -\frac{d\sqrt{2}}{2} & -\frac{d\sqrt{2}}{2} & -\frac{d\sqrt{2}}{2} & -\frac{d\sqrt{2}}{2} & \frac{d\sqrt{2}}{2} & \frac{d\sqrt{2}}{2} \\ \frac{d\sqrt{2}}{2} & \frac{d\sqrt{2}}{2} & \frac{d\sqrt{2}}{2} & \frac{d\sqrt{2}}{2} & -\frac{d\sqrt{2}}{2} & -\frac{d\sqrt{2}}{2} & -\frac{d\sqrt{2}}{2} & -\frac{d\sqrt{2}}{2} \\ j & -j & j & -j & -j & j & j & -j \end{bmatrix} \quad (35)$$

C.2 Hexarotor

Simple

The simple hexarotor control effectiveness matrix is shown in Equation 36.

$$B_f = \begin{bmatrix} 1 & 1 & 1 & 1 & 1 & 1 \\ 0 & -\frac{d\sqrt{3}}{2} & -\frac{d\sqrt{3}}{2} & 0 & \frac{d\sqrt{3}}{2} & \frac{d\sqrt{3}}{2} \\ d & \frac{d}{2} & -\frac{d}{2} & -d & -\frac{d}{2} & \frac{d}{2} \\ j & -j & j & -j & -j & j \end{bmatrix} \quad (36)$$

Coaxial

The coaxial hexarotor control effectiveness matrix is shown in Equation 37.

$$B_f = \begin{bmatrix} 1 & 1 & 1 & 1 & 1 & 1 & 1 & 1 & 1 & 1 & 1 & 1 \\ 0 & 0 & -\frac{d\sqrt{3}}{2} & -\frac{d\sqrt{3}}{2} & -\frac{d\sqrt{3}}{2} & -\frac{d\sqrt{3}}{2} & 0 & 0 & \frac{d\sqrt{3}}{2} & \frac{d\sqrt{3}}{2} & \frac{d\sqrt{3}}{2} & \frac{d\sqrt{3}}{2} \\ d & d & \frac{d}{2} & \frac{d}{2} & -\frac{d}{2} & -\frac{d}{2} & -d & -d & -\frac{d}{2} & -\frac{d}{2} & \frac{d}{2} & \frac{d}{2} \\ j & -j & -j & j & j & -j & -j & j & j & -j & -j & j \end{bmatrix} \quad (37)$$

C.3 Octorotor

Simple

The simple octorotor control effectiveness matrix is shown in Equation 38.

$$B_f = \begin{bmatrix} 1 & 1 & 1 & 1 & 1 & 1 & 1 & 1 \\ 0 & -\frac{d\sqrt{2}}{2} & -d & -\frac{d\sqrt{2}}{2} & 0 & \frac{d\sqrt{2}}{2} & d & \frac{d\sqrt{2}}{2} \\ d & \frac{d\sqrt{2}}{2} & 0 & -\frac{d\sqrt{2}}{2} & -d & -\frac{d\sqrt{2}}{2} & 0 & \frac{d\sqrt{2}}{2} \\ -j & j & -j & j & -j & j & -j & j \end{bmatrix} \quad (38)$$

Appendix D

DoC Configuration Analysis

The design requirements for this analysis are outline in Table D.1. The mass results of the configuration analysis are shown in Figure D.1, along the propeller diameter values shown in Table D.2. The results of this analysis can be found in the main body of the report, in Figure 3.5.

Table D.1: Design Requirements of DoC Configuration Analysis

Design Requirements	Value
Payload (kg)	2.5
Flight Time (min)	10
T/W	2
Climb Speed (m/s)	5
Flight Altitude (m)	30

Table D.2: Rotor Diameter of DoC Configuration Analysis

Configuration	Quadrotor	Hexarotor	Octorotor	Coaxial Quadrotor	Coaxial Hexarotor
Rotor Diameter (m)	0.55	0.46	0.43	0.43	0.36

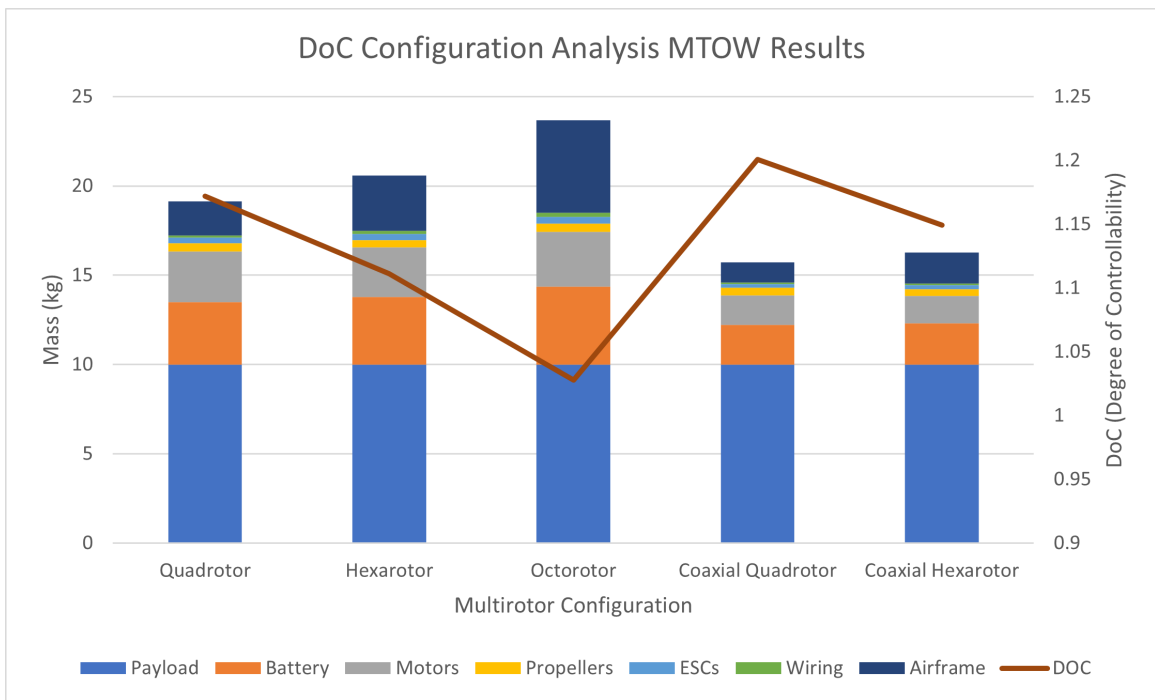


Figure D.1: DoC Configuration Analysis MTOW Results

Bibliography

- [1] “Phantom 4 - DJI.”
- [2] D. Raymer, *Aircraft Design: A Conceptual Approach, Sixth Edition*. Washington, DC: American Institute of Aeronautics and Astronautics, Inc., Sept. 2018.
- [3] W. Ong, S. Srigrarom, and H. Hesse, “Design Methodology for Heavy-Lift Unmanned Aerial Vehicles with Coaxial Rotors,” in *AIAA Scitech 2019 Forum*, (San Diego, California), American Institute of Aeronautics and Astronautics, Jan. 2019.
- [4] T. Schneider, G. Ducard, K. Rudin, and P. Strupler, “Fault-tolerant Control Allocation for Multirotor Helicopters Using Parametric Programming,” July 2012.
- [5] Q. Quan, *Introduction to multicopter design and control*. Springer, July 2017.
- [6] G. Klein, R. E. Lindberg, and R. W. Longman, “Computation of a degree of controllability via system discretization,” *Journal of Guidance, Control, and Dynamics*, vol. 5, pp. 583–588, Nov. 1982. Publisher: American Institute of Aeronautics and Astronautics.
- [7] S. Delbecq, M. Budinger, A. Ochotorena, A. Reysset, and F. Defay, “Efficient sizing and optimization of multirotor drones based on scaling laws and similarity models,” *Aerospace Science and Technology*, vol. 102, p. 105873, July 2020.
- [8] J. Liscouet, F. Pollet, J. Jézégou, M. Budinger, S. Delbecq, and J.-M. Moschetta, “A methodology to integrate reliability into the conceptual design of safety-critical multirotor unmanned aerial vehicles,” *Aerospace Science and Technology*, p. 107681, June 2022.

- [9] A. Bondyra, S. Gardecki, P. Gasiór, and W. Giernacki, “Performance of coaxial propulsion in design of multi-rotor uavs,” in *Challenges in Automation, Robotics and Measurement Techniques* (R. Szewczyk, C. Zieliński, and M. Kaliczyńska, eds.), (Cham), pp. 523–531, Springer International Publishing, 2016.
- [10] G.-X. Du and Q. Quan, “Optimization of Multicopter Propulsion System Based on Degree of Controllability,” *Journal of Aircraft*, vol. 56, pp. 2062–2069, Sept. 2019. Publisher: American Institute of Aeronautics and Astronautics.
- [11] J. Xu, “Design Perspectives on Delivery Drones,” tech. rep., RAND Corporation, Sept. 2017.
- [12] M. Rimjha, S. Hotle, A. Trani, and N. Hinze, “Commuter demand estimation and feasibility assessment for Urban Air Mobility in Northern California,” *Transportation Research Part A: Policy and Practice*, vol. 148, pp. 506–524, June 2021.
- [13] R. D’Andrea, “Guest Editorial Can Drones Deliver?,” *IEEE Transactions on Automation Science and Engineering*, vol. 11, pp. 647–648, July 2014. Conference Name: IEEE Transactions on Automation Science and Engineering.
- [14] N. Gunady, B. E. Sells, S. R. Patel, H. Chao, D. A. DeLaurentis, and W. A. Crossley, “Evaluating Future Electrified UAM-Enabled Middle-Mile Cargo Delivery Operations,” in *AIAA AVIATION 2022 Forum*, AIAA AVIATION Forum, American Institute of Aeronautics and Astronautics, June 2022.
- [15] S. Watkins, J. Burry, A. Mohamed, M. Marino, S. Prudden, A. Fisher, N. Kloet, T. Jakobi, and R. Clothier, “Ten questions concerning the use of drones in urban environments,” *Building and Environment*, vol. 167, p. 106458, Jan. 2020.
- [16] R. A. Clothier and R. A. Walker, “Safety Risk Management of Unmanned Aircraft Systems,” in *Handbook of Unmanned Aerial Vehicles* (K. P. Valavanis and G. J. Vachtsevanos, eds.), pp. 2229–2275, Dordrecht: Springer Netherlands, 2015.
- [17] S. B. Nazarudeen and J. Liscouët, “State-Of-The-Art And Directions For The Conceptual

- Design Of Safety-Critical Unmanned And Autonomous Aerial Vehicles,” in *2021 IEEE International Conference on Autonomous Systems (ICAS)*, pp. 1–5, Aug. 2021.
- [18] H. Hecht, *Systems Reliability and Failure Prevention*. Artech House, 2004. Google-Books-ID: iUEwDwAAQBAJ.
- [19] J. G. Leishman, *Principles of Helicopter Aerodynamics*. Cambridge University Press, Dec. 2016. Google-Books-ID: uscAMQAACAAJ.
- [20] C. Belcastro, R. Newman, J. Evans, D. Klyde, L. Barr, and E. Ancel, *Hazards Identification and Analysis for Unmanned Aircraft System Operations*. June 2017.
- [21] EASA, “Proposed means of compliance with the special condition vtol,” 2020.
- [22] “Guidelines for Development of Civil Aircraft and Systems,” *ARP4754 Rev A*, 2010.
- [23] J. Roskam, *Airplane Design: Preliminary sizing of airplanes*. DARcorporation, 1985. Google-Books-ID: usXVaf8Qu0cC.
- [24] P. Ngatchou, A. Zarei, and A. El-Sharkawi, “Pareto multi objective optimization,” in *Proceedings of the 13th International Conference on, Intelligent Systems Application to Power Systems*, pp. 84–91, 2005.
- [25] R. Warren and J. Liscouët, “Comparative analysis of sizing methodologies for high-reliability multicopters,” in *AIAA AVIATION 2022 Forum*, 2022.
- [26] M. Gatti, “Complete Preliminary Design Methodology for Electric Multirotor,” *Journal of Aerospace Engineering*, vol. 30, May 2017.
- [27] F. Bohorquez, D. Pines, and P. D. Samuel, “Small Rotor Design Optimization Using Blade Element Momentum Theory and Hover Tests,” *Journal of Aircraft*, vol. 47, pp. 268–283, Jan. 2010. Publisher: American Institute of Aeronautics and Astronautics.
- [28] J. Winslow, V. Hrishikeshavan, and I. Chopra, “Design Methodology for Small-Scale Unmanned Quadrotors,” *Journal of Aircraft*, vol. 55, no. 3, pp. 1062–1070,

2018. Publisher: American Institute of Aeronautics and Astronautics. eprint: <https://doi.org/10.2514/1.C034483>.
- [29] N. A. Vu, D. K. Dang, and T. Le Dinh, “Electric propulsion system sizing methodology for an agriculture multicopter,” *Aerospace Science and Technology*, vol. 90, pp. 314–326, July 2019.
- [30] L. Bauersfeld and D. Scaramuzza, “Range, Endurance, and Optimal Speed Estimates for Multicopters,” *IEEE Robotics and Automation Letters*, vol. 7, Apr. 2022.
- [31] E. L. de Angelis, F. Giulietti, G. Rossetti, and G. Bellani, “Performance analysis and optimal sizing of electric multirotors,” *Aerospace Science and Technology*, vol. 118, p. 107057, Nov. 2021.
- [32] C. Ampatis and E. Papadopoulos, “Parametric Design and Optimization of Multi-Rotor Aerial Vehicles,” in *Applications of Mathematics and Informatics in Science and Engineering* (N. J. Daras, ed.), Springer Optimization and Its Applications, pp. 1–25, Cham: Springer International Publishing, 2014.
- [33] D. Bershadsky, S. Haviland, and E. N. Johnson, “Electric Multirotor UAV Propulsion System Sizing for Performance Prediction and Design Optimization,” in *57th AIAA/ASCE/AHS/ASC Structures, Structural Dynamics, and Materials Conference*, AIAA SciTech Forum, American Institute of Aeronautics and Astronautics, Jan. 2016.
- [34] R. Gadekar, Abhishek, and M. Kothari, “Performance based systematic design methodology for development and flight testing of fuel engine powered quadrotor Unmanned Aerial System for industrial applications,” *Mechatronics*, vol. 82, p. 102722, Apr. 2022.
- [35] S. Oh, M. Kim, H. Kim, D. Lim, K. Yee, and D. Kim, “The Solution Development for Performance Analysis and Optimal Design of Multicopter-type Small Drones,” in *2020 International Conference on Unmanned Aircraft Systems (ICUAS)*, pp. 975–982, Sept. 2020. ISSN: 2575-7296.
- [36] G. Szafranski, R. Czyba, and M. BŁachuta, “Modeling and identification of electric propulsion

- system for multirotor unmanned aerial vehicle design,” in *2014 International Conference on Unmanned Aircraft Systems (ICUAS)*, pp. 470–476, May 2014.
- [37] L. N. Mascarello and F. Quagliotti, “Design of inoffensive sUAS for humanitarian missions,” *Aircraft Engineering and Aerospace Technology*, vol. 90, no. 3, pp. 524–531, 2018. Num Pages: 8 Place: Bradford, United Kingdom Publisher: Emerald Group Publishing Limited.
- [38] J. Ye, J. Wang, T. Song, Y. Zhu, Z. Wu, and P. Tang, “Propulsion optimization of a quadcopter in forward state,” *Aerospace Science and Technology*, vol. 113, p. 106703, June 2021.
- [39] S. K. Phang, K. Li, B. M. Chen, and T. H. Lee, “Systematic Design Methodology and Construction of Micro Aerial Quadrotor Vehicles,” *Handbook of Unmanned Aerial Vehicles*, pp. 181–206, 2015. Publisher: Springer, Dordrecht.
- [40] T. Ng and G. Leng, “Design of small-scale quadrotor unmanned air vehicles using genetic algorithms,” *Proceedings of The Institution of Mechanical Engineers Part G-journal of Aerospace Engineering - PROC INST MECH ENG G-J A E*, vol. 221, pp. 893–905, May 2007.
- [41] Magnussen, M. Ottestad, and G. Hovland, “Multicopter Design Optimization and Validation,” *Modeling, Identification and Control: A Norwegian Research Bulletin*, vol. 36, pp. 67–79, Apr. 2015.
- [42] V. M. Arellano-Quintana, E. A. Portilla-Flores, E. A. Merchan-Cruz, and P. A. Niño-Suarez, “Multirotor design optimization using a genetic algorithm,” in *2016 International Conference on Unmanned Aircraft Systems (ICUAS)*, pp. 1313–1318, June 2016.
- [43] T. Du, A. Schulz, B. Zhu, B. Bickel, and W. Matusik, “Computational multicopter design,” *ACM Transactions on Graphics*, vol. 35, pp. 227:1–227:10, Nov. 2016.
- [44] M. Biczyski, R. Sehab, J. F. Whidborne, G. Krebs, and P. Luk, “Multirotor Sizing Methodology with Flight Time Estimation,” *Journal of Advanced Transportation*, vol. 2020, p. 14, Jan. 2020. Publisher: Hindawi.
- [45] A. Ayaz and A. Rasheed, “Multi-Objective Design Optimization of Multicopter using Genetic

- Algorithm,” in *2021 International Bhurban Conference on Applied Sciences and Technologies (IBCAST)*, pp. 177–182, Jan. 2021. ISSN: 2151-1411.
- [46] X. Dai, Q. Quan, J. Ren, and K.-Y. Cai, “An Analytical Design-Optimization Method for Electric Propulsion Systems of Multicopter UAVs With Desired Hovering Endurance,” *IEEE/ASME Transactions on Mechatronics*, vol. PP, pp. 1–1, Jan. 2019.
- [47] X. Dai, Q. Quan, and K.-Y. Cai, “Design Automation and Optimization Methodology for Electric Multicopter Unmanned Aerial Robots,” *IEEE Transactions on Automation Science and Engineering*, pp. 1–15, 2021. Conference Name: IEEE Transactions on Automation Science and Engineering.
- [48] “flyeval - Flight Performance Evaluation of UAVs.”
- [49] P. M. Renkert and A. G. Alleyne, “Component-Based Design Optimization of Multirotor Aircraft,” in *2022 American Control Conference (ACC)*, pp. 3985–3990, June 2022. ISSN: 2378-5861.
- [50] M. Achtelik, K.-M. Doth, D. Gurdan, and J. Stumpf, “Design of a Multi Rotor MAV with regard to Efficiency, Dynamics and Redundancy,” in *AIAA Guidance, Navigation, and Control Conference*, American Institute of Aeronautics and Astronautics, 2012. eprint: <https://arc.aiaa.org/doi/pdf/10.2514/6.2012-4779>.
- [51] P. M. Basset, A. Tremolet, and T. Lefebvre, “Rotary Wing UAV pre-sizing : Past and Present Methodological Approaches at Onera,” *Aerospace Lab*, no. 8, p. 1, 2014.
- [52] L. Rana, T. McCall, J. Haley, L. Gonzalez, A. Omoragbon, A. Oza, and B. Chudoba, “A Paradigm-Shift in Aerospace Vehicle Design Synthesis and Technology Forecasting,” in *2018 AIAA SPACE and Astronautics Forum and Exposition*, American Institute of Aeronautics and Astronautics, 2018. eprint: <https://arc.aiaa.org/doi/pdf/10.2514/6.2018-5210>.
- [53] A. Lambe and J. Martins, “Extensions to the Design Structure Matrix for the Description of Multidisciplinary Design, Analysis, and Optimization Processes,” *Structural and Multidisciplinary Optimization*, Aug. 2012.

- [54] J. S. Gray, J. T. Hwang, J. R. R. A. Martins, K. T. Moore, and B. A. Naylor, “OpenMDAO: An open-source framework for multidisciplinary design, analysis, and optimization,” *Structural and Multidisciplinary Optimization*, vol. 59, pp. 1075–1104, April 2019.
- [55] R. E. Kalman, “Contributions to the theory of optimal control,” *Bol. soc. mat. mexicana*, vol. 5, no. 2, pp. 102–119, 1960.
- [56] N. S. Nise, *Control Systems Engineering*. John Wiley & Sons, June 2020. Google-Books-ID: sEL2DwAAQBAJ.
- [57] S. Sun, M. Baert, B. Schijndel, and C. De Visser, “Upset recovery control for quadrotors subjected to a complete rotor failure from large initial disturbances,” pp. 4273–4279, 05 2020.
- [58] J. Zhang, M. Söpper, and F. Holzapfel, “Attainable moment set optimization to support configuration design: A required moment set based approach,” *Applied Sciences*, vol. 11, no. 8, 2021.
- [59] M. Saied, H. Shraim, C. Francis, I. Fantoni, and B. Lussier, “Controllability analysis and motors failures symmetry in a coaxial octorotor,” in *2015 Third International Conference on Technological Advances in Electrical, Electronics and Computer Engineering (TAECE)*, pp. 245–250, Apr. 2015.
- [60] A. Sanjuan, F. Nejjari, and R. Sarrate, “Reconfigurability Analysis of Multirotor UAVs under Actuator Faults,” in *2019 4th Conference on Control and Fault Tolerant Systems (SysTol)*, pp. 26–31, Sept. 2019. ISSN: 2162-1209.
- [61] C. N. Viswanathan, R. W. Longman, and P. W. Likins, “A degree of controllability definition - Fundamental concepts and application to modal systems,” *Journal of Guidance, Control, and Dynamics*, vol. 7, pp. 222–230, Mar. 1984. Publisher: American Institute of Aeronautics and Astronautics.
- [62] D. Shi, B. Yang, and Q. Quan, “Reliability analysis of multicopter configurations based on controllability theory,” in *2016 35th Chinese Control Conference (CCC)*, pp. 6740–6745, July 2016. ISSN: 1934-1768.

- [63] G.-X. Du, Q. Quan, B. Yang, and K.-Y. Cai, “Controllability Analysis for Multirotor Helicopter Rotor Degradation and Failure,” *Journal of Guidance, Control, and Dynamics*, vol. 38, pp. 978–985, May 2015.
- [64] G. Ortiz-Torres, P. Castillo, F. D. J. Sorcia-Vázquez, J. Y. Rumbo-Morales, J. A. Brizuela-Mendoza, J. De La Cruz-Soto, and M. Martínez-García, “Fault estimation and fault tolerant control strategies applied to vtol aerial vehicles with soft and aggressive actuator faults,” *IEEE Access*, vol. 8, pp. 10649–10661, 2020.
- [65] B. Yang, G. Du, Q. Quan, and K.-Y. Cai, “The degree of controllability with limited input and an application for hexacopter design,” in *Proceedings of the 32nd Chinese Control Conference*, pp. 113–118, July 2013. ISSN: 1934-1768.
- [66] C. David, S. Delbecq, S. Defoort, P. Schmollgruber, E. Benard, and V. Pommier-Budinger, “From FAST to FAST-OAD: An open source framework for rapid overall aircraft design,” *IOP Conference Series: Materials Science and Engineering*, vol. 1024, p. 012062, jan 2021.